Impact of Land Use and Land Cover Changes on Ecosystem Services: A Multi-Module InVEST-LCM Analysis

Fahad Hasan [a]* 0009-0009-7824-5538, Yashar Makhtoumi [b] 0000-0002-0305-6849, Gang Chen [a] 0000-0002-6476-7812

[a] Department of Civil and Environmental Engineering, Florida State University, Tallahassee, FL 32310, USA a
[b] Center for Sustainability and the Global Environment, Nelson Institute for Environmental Studies, University of Wisconsin-Madison, Madison, WI 53726, USA b

* Correspondence: Fahad Hasan, fh23b@fsu.edu

Abstract

Land use and land cover (LULC) dynamics influence ecological processes and the provision of essential ecosystem services (ESs). So, understanding how LULC changes influence ESs is critical for sustainable land management and conservation planning, especially in rapidly urbanizing watersheds. Despite studies examining individual ecosystem services, there remains a notable research gap in comprehensive, spatially explicit analyses integrating multiple ESs across historical and projected timelines. This study addresses this gap by assessing the impacts of historical and projected LULC changes on multiple ESs in the Hillsborough River Watershed in Florida, USA, from 2000 through projected scenarios to 2050. Using a combination of remote sensing data, the Land Change Modeler (LCM) within TerrSet software, and the Integrated Valuation of Ecosystem Services and Tradeoffs (InVEST) model, we quantified and projected changes in six ESs: annual water yields, flood mitigation, carbon storage, nutrient retention, sediment export, and recreational visitation. Additionally, ecosystem service values (ESVs) were economically assessed using inflation-adjusted global valuation coefficients. Results revealed that from 2000 to 2023, urban land expanded by over 30%, primarily replacing croplands, wetlands, and forests. This urbanization reduced carbon storage by 11.8% and runoff retention by 4.6%, while sediment export increased by 9.4%. The total ESV declined by approximately $450 million, highlighting substantial ecological and economic losses. Projected scenarios indicated continued urban growth by 2050, with urban areas potentially occupying nearly half of the watershed. This expansion would further reduce carbon storage by an additional 11.1%, runoff retention by 2.9%, and sediment export 10.9%. Consequently, cumulative ESV losses are projected to surpass $1 billion by 2050. These findings underscore the urgent need for integrating ecosystem-based conservation strategies into urban policy frameworks. By adopting proactive measures that prioritize high-value natural areas and promote ecological restoration, stakeholders can better balance urban growth with environmental sustainability ensuring long-term resilience for both natural and human communities.

Keywords: Land-use/land-cover change; Urban expansion; Ecosystem service; InVEST model; Land Change Modeler; Watershed management

Highlights

- Urban areas increased by about 31%, driving declines in forest, cropland, and wetland cover.
- The InVEST model assessed changes in six ecosystem services under historical and projected LULC scenarios.
- A CA-Markov–MLP integrated LCM approach was used to simulate future land use dynamics.
- Urbanization led to declines in carbon storage and runoff retention, but increases in water yield and sediment export.
- Land use changes from 2000 to 2050 led to a 1.02 billion USD decline in ecosystem service value.

Graphical Abstract

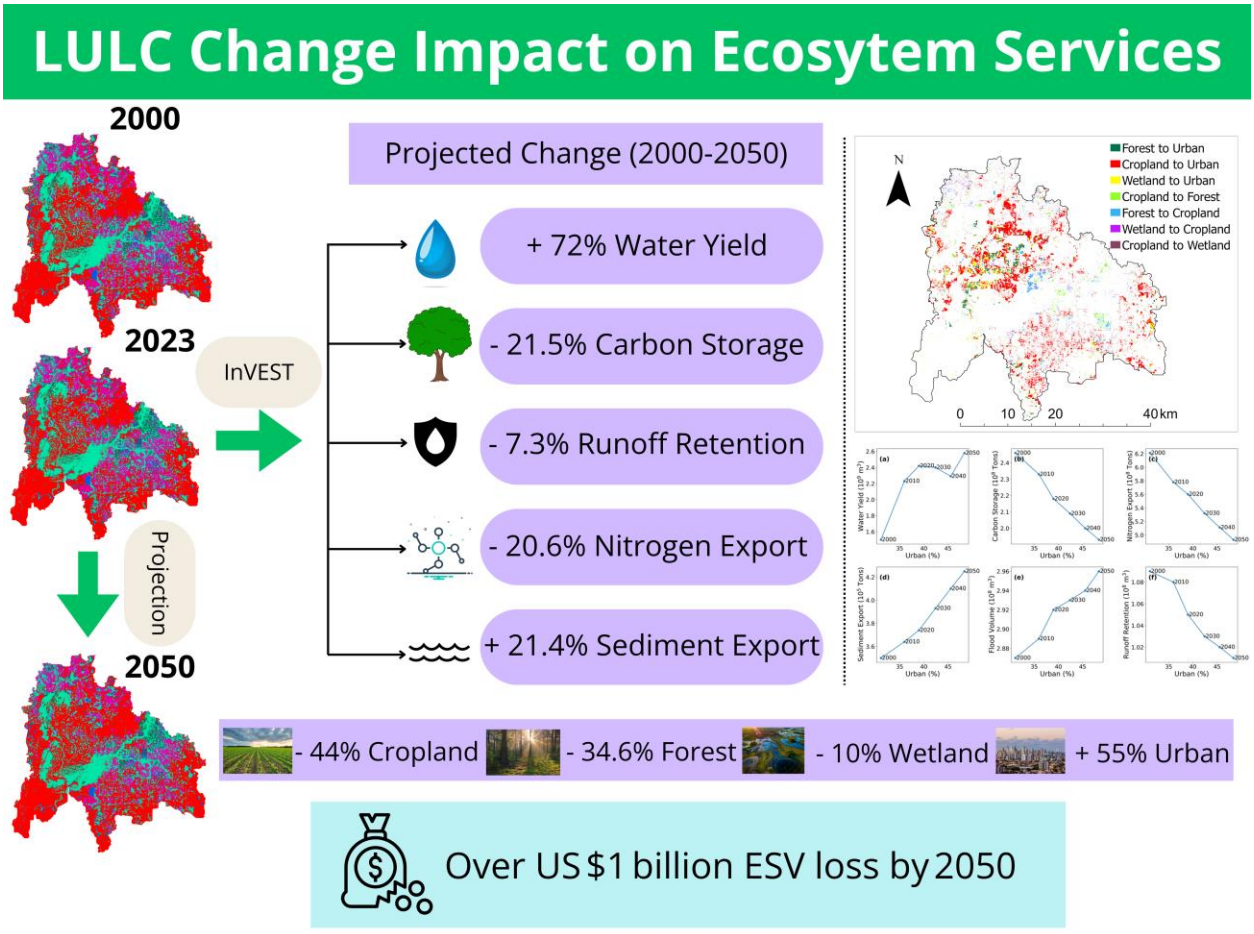

Graphical abstract descriptions: This graphical abstract provides a summary of the study on the impacts LULC change on ESs in the Hillsborough River Watershed from 2000 to 2050. The left panel illustrates the

temporal sequence of classified LULC maps for 2000, 2023, and projected 2050. These maps highlight a substantial increase in urban areas alongside declines in cropland, forest, and wetland extents. These LULC transitions were modeled using the TerrSet-LCM, employing Multi-Layer Perceptron (MLP) and Markov chain-based simulations. Their effects on ecosystem services were quantified using InVEST modules.

Central to the abstract is a synthesis of projected outcomes between 2000 and 2050. The results indicate a 72% increase in water yield and a 21.4% rise in sediment export, contrasted by declines in carbon storage (−21.5%), nitrogen export (−20.6%), and runoff retention (−7.3%). These values reflect the trade-offs associated with urbanization, driven by the loss of natural and agricultural land covers. The top-right panel displays spatial patterns of dominant LULC transitions, such as cropland-to-urban and forest-to-urban conversions, while the bottom-right panel presents the relationships between urban expansion and ecosystem service indicators. Collectively, the results indicate that by 2050, a 55% increase in urban land, coupled with a 44% reduction in cropland, 34.6% reduction in forest, and 10% loss in wetlands, could lead to an overall ecosystem service value loss exceeding US $1 billion.

1. Introduction

Land use and land cover (LULC) changes are among the most influential drivers of environmental transformation. These changes directly affect the capacity of landscapes to provide essential ecosystem services (ESs) (Biedemariam et al., 2022). ESs underpin environmental stability by providing, regulating, supporting, and enriching human well-being while sustaining community development (Jiang et al., 2021; Torres et al., 2021). For instance, regulating services such as water cycle management and carbon sequestration help maintain ecological balance (Petsch et al., 2023), while supporting services such as soil stabilization and biodiversity conservation ensure long-term ecosystem resilience (Lal et al., 2021). However, when natural ecosystems such as forests and wetlands are converted into agricultural land, urban areas, or industrial sites, their ability to maintain these functions declines (Liu & Wu, 2022; Schirpke et al., 2023).

Certain changes, such as afforestation and ecological restoration, may enhance ES provision. However, most transformations-particularly deforestation, agricultural expansion, and urbanization are associated with substantial ES losses. Among these transformations, urbanization is one of the fastest-growing forms of land change. Rapid urban growth, driven by population expansion, infrastructure development, and changing land use priorities, often results in pronounced environmental disruptions (Fang et al., 2022). Key ESs such as hydrological regulation, carbon storage, nutrient retention, sediment transport, and flood mitigation are particularly affected (Guo et al., 2021; Xiao et al., 2023).

Conversion of permeable landscapes to impervious surfaces increases surface runoff, reduces groundwater recharge, and degrades water quality, thereby elevating flood risks (Lu et al., 2022; Sun et al., 2023). Likewise, the replacement of forests and croplands with built-up areas diminishes carbon sequestration capacity, contributing to climate change (X. Li et al., 2022). Although green infrastructure and afforestation initiatives have been introduced to counteract these effects, they often fall short of offsetting the ecological losses linked to unplanned urban expansion (Mohammadyari et al., 2023).

Over the past decade, researchers have increasingly focused on integrating ES assessments into land use planning, supported by advancements in remote sensing, spatial modeling, and valuation techniques (L. Li et al., 2022; Y. Li et al., 2023; Yu et al., 2022). Recent studies have also emphasized multi-service evaluation frameworks, such as the use of remote sensing combined with modeling tools, to assess the cumulative impacts of LULC changes on ES provision (Gomes et al., 2021; Jian et al., 2024; R. Wang et al., 2022; Zarandian et al., 2023). Zhu et al. (2024) linked Patch-generating Land Use Simulation (PLUS) model with InVEST to examine water-carbon-land dynamics under alternative policy scenarios. Complementing this,

Aghaloo & Sharifi (2025) combined PLUS with multiple InVEST modules to compare urban development scenarios in Tehran, quantifying trade-offs among seven Ess.

Despite these advances, knowledge gaps remain. Many studies assess individual ESs in isolation, such as carbon sequestration or water regulation (Ismaili Alaoui et al., 2023; Nahib et al., 2021), which lacks comprehensive and integrated assessment of land use impacts on ecosystem functioning. In addition, much of the existing research lacks continuity across historical and projected time horizons, making it difficult to evaluate long-term trade-offs. Furthermore, there is a shortage of spatially explicit, multi-decadal analyses in humid subtropical regions to examine multiple ESs. Addressing these gaps requires an approach that integrates remote sensing, land change modeling, and ES quantification in a consistent framework, applied over both past and projected timelines.

In response, the present study applies modeling approach to quantify and project the effects of LULC changes on multiple Ess across the Hillsborough River Watershed in Florida, USA, from 2000 through 2050. Specifically, this research aims to (1) analyze LULC dynamics from 2000 to 2023 and simulate future land use scenarios for 2030, 2040, and 2050 using remote sensing and land change modeling techniques, and (2) quantify the effects of LULC changes on multiple Ess (annual water yields, runoff retention, flood volume, carbon storage, nutrient exports- nitrogen and phosphorus, sediment delivery, and recreational visitation) and their economic values, providing an integrated perspective that can inform sustainable watershed management and urban planning.

2. Materials and Methods

2.1. Study area

The study focuses on the Hillsborough River Watershed, located in Tampa, Florida (**Figure 1**). This watershed is classified as a Hydrologic Unit Code (HUC) subbasin, specifically a HUC-8 (03100205). HUCs are part of a national watershed classification system developed by the U.S. Geological Survey (USGS) and the U.S. Department of Agriculture (USDA). A HUC-8 represents a subbasin level of delineation, providing a standardized unit for analyzing and managing water resources. The Hillsborough River watershed is about 1,700 square kilometers. This watershed has a humid subtropical climate, with hot, humid summers and mild winters. Temperatures remain relatively consistent throughout the year, ranging from 18°C to 35°C. The watershed receives an average annual precipitation of 1,295 mm, with recorded variations ranging from 813 mm in dry years to 1,956 mm in wet years. Elevations range from sea level to around 85 m, with higher terrain in the southeast and northeast.

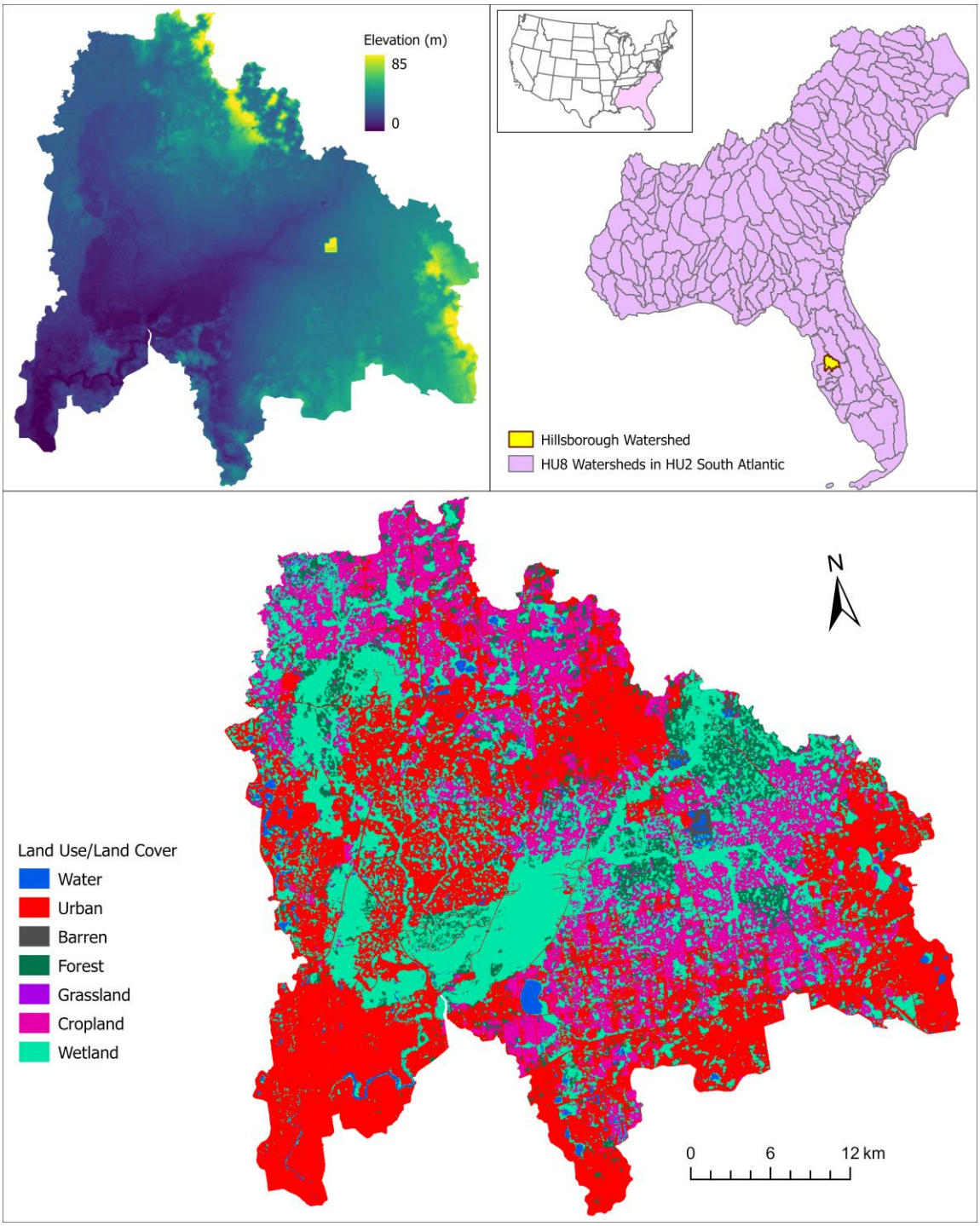

Figure 1: Location of Hillsborough River Watershed. It is a HUC-8 watershed located in Tampa, Florida. The elevation ranges from 0 to 85 meters, with the highest elevated areas located in the southeast and northeast regions. Urban, wetland and cropland are the most dominant land types.

The watershed is urbanized, with urban areas occupying roughly 40% of the land area, while natural land covers such as wetlands, forests, and grasslands remain in the rest (**Table 1**).

Table 1: Area and Percentage of Land Use and Land Cover Classes in the Hillsborough River Watershed

Land Use Class	Area (ha)	Percentage of Total Area (%)
Water	2930.04	1.72
Urban	69068.07	40.64
Barren	753.39	0.44
Forest	11515.77	6.78
Grassland	245.97	0.14
Cropland	35351.19	20.80
Wetland	50072.13	29.47

These natural areas provide essential ecosystem services (ESs) including water filtration, flood control, carbon sequestration, and habitat provision. The region also supports diverse recreational activities such as fishing and boating. Sociodemographic trends indicate notable population growth over recent decades. The watershed's population increased from 42,862 in 1970 to a peak of 197,952 in 2010, before declining to 145,034 in 2020. This demographic change reflects the impacts of urban expansion, shifting land use, and development pressures.

2.2. Data Sources

The data used in this study were obtained from sources summarized in **Table 2** for the years 2000, 2005, 2010, 2015, 2020, and 2023, which also includes their respective spatial resolutions.

Table 2: Input data sources, resolution, and applications for InVEST and LCM models

InVEST Model				
Parameter	**Resolution**	**Unit**	**Source**	**Application**
Land use maps	30 m	LULC Classification	National Land Cover Database (www.mrlc.gov)	Input for every ES module
Digital Elevation Model (DEM)	30 m	m	United States Geological Survey (www.usgs.gov)	Nutrient and Sediment delivery module
Hydrologic Soil Groups	30 m	A–D categories	SSURGO (www.nrcs.usda.gov)	Flood Mitigation module
Precipitation (Historical)	4 km	mm/year	PRISM climate group (https://prism.oregonstate.edu/)	Water yield, flood mitigation, and NDR modeling

Future Precipitation (CMIP6)	5 km	mm/year	NASA NEX-GDDP CMIP6 (https://www.nccs.nasa.gov)	Future ES projections in InVEST (water yield, flood mitigation, NDR)
Parameter	**Resolution**	**Unit**	**Source**	**Application**
Evapotranspiration	1 km	mm/year	United States Geological Survey (www.usgs.gov)	Water yield module
Root Restricting Layer Depth	1 km	mm	Harmonized World Soil Database (HWSD) (http://webarchive.iiasa.ac.at)	Water yield module
Plant Available Water Content	1 km	dimensionless fraction	Harmonized World Soil Database (HWSD) (http://webarchive.iiasa.ac.at)	Water yield module
Rainfall Erosivity	800 m	MJ · mm/ (h · ha · year)	NOAA (https://www.fisheries.noaa.gov)	SDR module
Soil Erodibility	30 m	t · h · ha / (ha · MJ · mm)	USDA gNATSGO (https://www.nrcs.usda.gov)	SDR module
Land Use Simulation Model (LCM-TerrSet)				
Land use maps	30 m	LULC Classification	National Land Cover Database (www.mrlc.gov)	Historical land use mapping and classification for baseline and transition analysis
Digital Elevation Model (DEM)	30 m	m	United States Geological Survey (www.usgs.gov)	Slope and elevation analysis for suitability mapping
Road Network	30 m	m	Open street map (https://www.openstreetmap.org/)	Accessibility and proximity analysis influencing urban expansion patterns
Urban Proximity	30 m	m	Open street map (https://www.openstreetmap.org/)	Proximity factor in land use change modeling to capture urban growth trends

All spatial datasets collected from various sources were processed to ensure consistency in spatial resolution and projection. Raster datasets with differing resolutions were resampled to a uniform 30 m × 30 m grid, matching the resolution of the NLCD land use data. This homogenization facilitated seamless integration and analysis across the InVEST and LCM–TerrSet models, ensuring spatial comparability and accuracy in subsequent modeling steps.

The methodology follows a staged workflow. Historical LULC (2000–2023) was mapped and change was quantified. Using the driving factors such as urban and road proximity, TerrSet's LCM with a CA-Markov routine was then used to project LULC for 2030, 2040, and 2050. Next, six InVEST modules-Water Yield, Carbon Storage, Nutrient Delivery Ratio, Sediment Delivery Ratio, Urban Flood Risk Mitigation, and

Recreation-were run using historical and projected LULC along with other input data (e.g. DEM, precipitation). Outputs were converted to monetary values (ESV) using global coefficient and adjusted to 2024 USD with CPI.

The Methodological framework for this study is demonstrated in **Figure 2.**

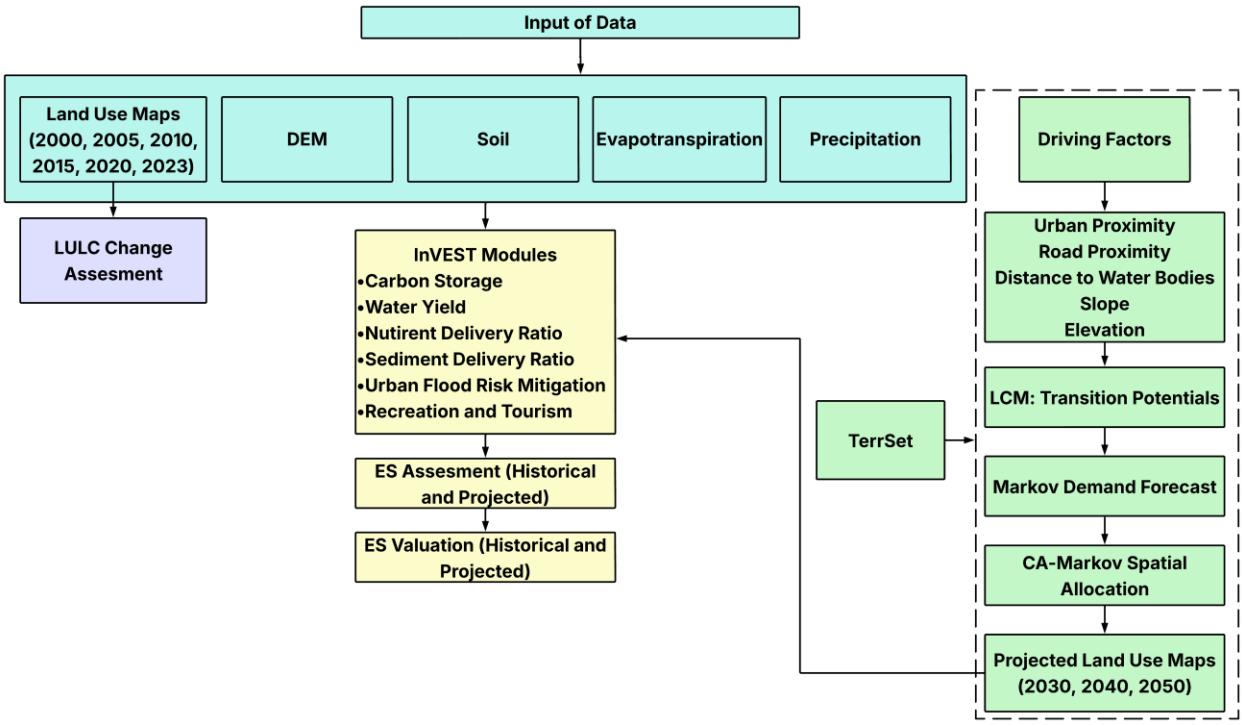

Figure 2: Workflow diagram of the integrated methodology used in this study. The framework combines observed land use maps, biophysical datasets (DEM, soil, precipitation, evapotranspiration), and driving factors to assess historical changes and project future land use scenarios using TerrSet's CA-Markov model. Projected land use maps (2030, 2040, 2050) were then used as inputs for InVEST modules (e.g., Carbon Storage, Water Yield, Nutrient Delivery, Sediment Delivery, Flood Mitigation, and Recreation) to quantify ES and ESV.

2.3. InVEST Model

The InVEST model is a spatially explicit tool developed by the Natural Capital Project, a partnership among Stanford University, the University of Minnesota, The Nature Conservancy, and the World Wildlife Fund. The project aims to advance ecosystem service science and provide practical tools that help integrate the value of nature into decision-making. The InVEST analysis in this study was performed using 30 m resolution rasters, covering approximately 1.8 billion cells across the watershed. On a standard workstation, InVEST modules ran in 5-10 minutes each, with the full workflow requiring several hours per scenario. Six modules consisting of annual water yields, carbon storage, nutrient delivery ratio, sediment delivery ratio,

urban flood risk mitigation, and visitation: recreation and tourism were used. These modules were chosen because they represent the most relevant ecosystem services for an urbanizing watershed. They also align with policy and planning concerns such as water regulation, carbon storage, and flood mitigation and could be reliably parameterized with the available datasets.

2.3.1 Carbon Storage:

The InVEST Carbon Storage Module was utilized to estimate the amount of carbon stored in the landscape. This module considers four primary carbon pools: aboveground biomass, belowground biomass, soil organic matter, and dead organic matter. The carbon density values for the chosen land types were taken from existing literature (Publications - IPCC-TFI, 2006; Smith et al., 2006; Tilman et al., 2006).

2.3.2 Water Yields:

The water yields in this study were estimated using the InVEST Annual Water Yield module. This module estimates annual yield per pixel using a Budyko-based water balance (Gan et al., 2021; C. Wang et al., 2016), where precipitation inputs are reduced by evapotranspiration determined from climate, soil, and vegetation characteristics. Results are then aggregated to the sub watershed scale. The model calculates the annual water yields (P_{xj}) for each pixel x based on land use and climate conditions as follows:

$$P_{xj} = \left(1 - \frac{AET_{xj}}{P_x}\right) \cdot P_x \text{.....(1)}$$

where AET_{xj} represents actual evapotranspiration, and P_x is the annual precipitation for pixel x.

2.3.3 Nutrient Delivery Ratio:

The total nitrogen and total phosphorus exports in this study were estimated using the Nutrient Delivery Ratio (NDR) module of the InVEST model. The model quantifies nutrient exports by computing the nutrient load for each pixel and applying a delivery ratio that accounts for topographical and hydrological characteristics (Redhead et al., 2018). The total nutrient export is calculated using the formula:

$$x_{\exp_i} = \text{load}_{\text{surf},i} \times \text{NDR}_{\text{surf},i} + \text{load}_{\text{subs},i} \times \text{NDR}_{\text{subs},i} \quad \text{..... (2)}$$

where $x_{\exp_i}$ represents the nutrient exports from pixel i, $\text{load}_{\text{surf},i}$ and $\text{load}_{\text{subs},i}$ denote the surface and subsurface nutrient loads, and $\text{NDR}_{\text{surf},i}$ and $\text{NDR}_{\text{subs},i}$ are the corresponding nutrient delivery ratios. The estimated total nutrient export was calculated by summing the contributions from all pixels:

$$x_{\exp_{\text{tot}}} = \sum_i x_{\exp_i} \text{ ..... (3)}$$

2.3.4 Sediment Delivery Ratio:

The sediment delivery and retention in the study area were assessed using the InVEST Sediment Delivery Ratio (SDR) module, which estimates soil loss and sediment exports based on land use and biophysical parameters. The module calculates annual soil loss ($usle_i$) using the Revised Universal Soil Loss Equation (RUSLE):

$$usle_i = R_i \cdot K_i \cdot LS_i \cdot C_i \cdot P_i \quad \text{(4)}$$

where R_i is the rainfall erosivity factor, K_i is the soil erodibility factor, LS_i represents the slope length-gradient factor, C_i is the cover management factor, and $P_i$is the support practice factor. The sediment export E is then computed as:

$$E = \sum_i usle_i \cdot SDR_i \quad \text{(5)}$$

where SDR_i is the sediment delivery ratio which represents the fraction of eroded soil reaching the stream. Default model parameters values were used for the cover management factor and support practice factor due to absence of local values.

2.3.5 Urban Flood Risk Mitigation:

The urban flood risk mitigation tool from the InVEST model was used for runoff retention and flood volume of the watershed. The InVEST model estimates the runoff production using the Curve Number method (Forootan, 2023; Munna et al., 2021), given by:

$$Q_{p,i} = \frac{\left(P - \lambda S_{\max,i}\right)^2}{P + (1-\lambda) S_{\max,i}} \quad \text{(6)}$$

where $Q_{p,i}$ represents the runoff per pixel, P is the storm depth, $S_{\max,i}$ is the potential retention, and λ. $S_{\max,i}$ is initial abstraction (λ = 0.2 for simplification). The model also computes runoff retention R_i as:

$$R_i = 1 - \frac{Q_{p,i}}{P} \quad \text{(7)}$$

which quantifies the retained stormwater in urban environments, aiding decision-making for flood control strategies.

2.3.6. Recreation and Tourism:

Lastly, the number of recreational visitations was determined by using the visitation: recreation and tourism module of the InVEST model. This module estimates the spatial distribution of recreational activity, measured in person-days, based on the presence and extent of natural and built features that influence where people choose to recreate. Due to the frequent lack of empirical visitation data, the model uses a proxy, photo-user-days (PUDs). The module predicts visitation patterns using a regression model:

$$y_i = \beta_0 + \beta_1 x_{i1} + \cdots + \beta_p x_{ip} \quad \ldots\ldots\ldots\ldots\ldots\ldots (8)$$

where y_i is the log-transformed average number of PUDs for each grid cell or polygon, x_{ip} is the value of predictor variable p in cell i, and β_p is the estimated effect of that variable on visitation.

2.4. Global and Adjusted ESV

The global ESV used in this study was based on the widely recognized coefficients provided by Costanza et al. (2014). These coefficients quantify the monetary value of ESs for land cover types in terms of US$ per hectare per year. They represent a global benchmark for evaluating the contributions of ecosystems to human well-being. For this analysis, the original value coefficients from 2007 were used as a starting point.

To ensure the relevance of these coefficients was in the context of the present study and current economic conditions, the values were adjusted to 2024 equivalents. The adjustment accounted for inflation and changes in the Consumer Price Index (CPI). The CPI values were taken from US bureau of labor statistics (https://www.bls.gov/) and the formula used for this conversion is as follows:

$$\text{Adjusted Value (2024)} = \text{Value (2007)} \times \frac{\text{CPI(2024)}}{\text{CPI(2007)}} \quad \ldots\ldots\ldots\ldots\ldots (9)$$

This adjustment ensures that the ES values reflect the current economic conditions and purchasing power. The adjusted coefficients were subsequently applied to the LULC maps for the Hillsborough River Watershed to calculate the total ESV for each period. For that, the overall ecosystem service value for each LULC type was calculated by multiplying the area of each LULC type in hectares by its corresponding value coefficient.

$$ESV = \sum(A_K \times VC_k) \quad \ldots\ldots\ldots\ldots\ldots (10)$$

ESV is the total estimated ecosystem service value, where VC_k is the value coefficient (US$ ha^{-1} year^{-1}) for LULC type ‘k', A_k is the area (ha), and ESV is the total estimated ecosystem service value.

2.5. Land Use Prediction

TerrSet, (an integrated geospatial software system for monitoring and modeling the earth system for sustainable development), particularly its Land Change Modeler (LCM) tool, was employed for this study. This model enables researchers to analyze land use changes, model transition potentials, and predict future land cover scenarios (Abolmaali et al., 2024; Bradley et al., 2017; Guder & Kabeta, 2025). In this study, LCM was used to project land use for the year 2030, 2040, and 2050. First, classified land cover maps for two time points (2000 and 2020) were taken and ensured they were aligned and consistently categorized. Then they were analyzed with LCM's Change Analysis module to quantify gross gains, losses, and category-to-category transitions (e.g., forest → cropland).

To discover where change is most likely, Transition Potential Models (TPMs) were built. LULC transitions that shared similar underlying mechanisms were grouped into separate transition sub-models. For each sub-model candidate, driver variables were assembled spanning biophysical and proximity factors (i.e., slope, elevation, and distance to road and towns). Driver significance was tested with Cramer's V and only variables exhibiting a meaningful association with observed change were retained. Transition potentials were then estimated with a Multi-Layer Perceptron (MLP) neural network. MLP was selected over SimWeight and logistic regression because of its ability to capture complex, non-linear relationships and to handle multiple transitions simultaneously. The MLP outputs continuous suitability maps (0–1), indicating each pixel's likelihood of undergoing a specific transition. A Markov chain was then applied to the 2000 – 2020 transition matrix Tij, where each element records the chance that a pixel of class i becomes class j. In compact form,

$$S(t+1) = TijxS(t) \dots\dots\dots\dots\dots\dots\dots \quad (11)$$

$$\mathrm{T}ij = \begin{bmatrix} \mathrm{T}11 & \mathrm{T}12 & \dots & \mathrm{T}1n \\ T21 & T2 & \dots & T2n \\ \vdots & \vdots & \dots & \vdots \\ \mathrm{T}n1 & \mathrm{T}n2 & \dots & \mathrm{T}nn \end{bmatrix} (0 \le \rho\mathrm{ij} \le 1) \dots\dots\dots\dots\dots\dots\dots (12)$$

where S(t) is the land-cover map (or state vector) at time t, S (t + 1) is its projection one step ahead, and Tij is the transition-probability matrix specifying the likelihood that a pixel presently in class i will convert to class j.

The model estimated the expected area or demand for each land-cover class at future time steps. The approach assumes that historical transition rates offer a reasonable first-order approximation of how land cover changes in the near future. The projected demands were then spatially distributed with TerrSet's stochastic CA-Markov routine. The cellular automata (CA) component applies neighborhood rules in a 5 × 5 window to reproduce the spatial contagion of LULC patches, while the Markov component governs

the probability of each pixel changing from class i to j over the chosen time step. A projection map for 2023 was also produced and compared with the observed 2023 map. The resulting overall kappa coefficient, $\kappa = 0.94$ (Text S3), indicated excellent agreement, giving confidence in the 2030, 2040 and 2050 forecasts. Throughout the projection workflow, protected areas were treated as immutable constraints, ensuring that legally conserved pixels did not transition.

3. Results

3.1. LULC Changes

The Hillsborough River watershed has undergone LULC changes from 2000 to 2023, characterized by urbanization and a decline in cropland, forests, and wetlands (**Figure 3)**. Urban areas expanded dramatically, increasing from 52,885 hectares in 2000 to 69,068 hectares in 2023, representing a growth of over 30%. In contrast, cropland exhibited a steady decline, decreasing from nearly 30% to around 22%.

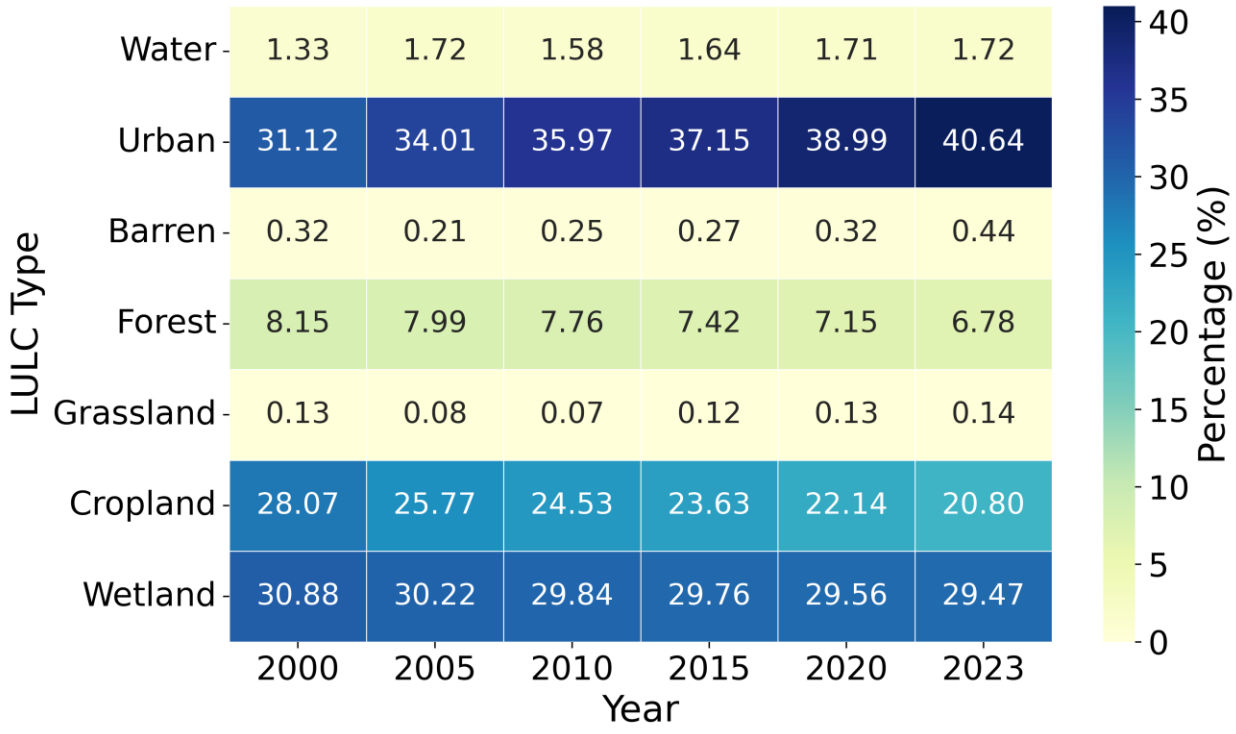

Figure 3: LULC changes between 2000 and 2023 in percentage. Urban areas experienced a notable increase, while the cropland, wetland, and forest decreased. Other land types such as barren and grassland showed similar change.

Forests decreased about 17% between 2000 and 2023 to become 6.78% of the total area in 2023. Furthermore, grassland, although smaller in extent, showed fluctuations, with a slight increase from 217

hectares in 2000 to 245 hectares in 2023. Water bodies, meanwhile, showed minor changes, increasing from 2,258 hectares to 2,930 hectares over the study period.

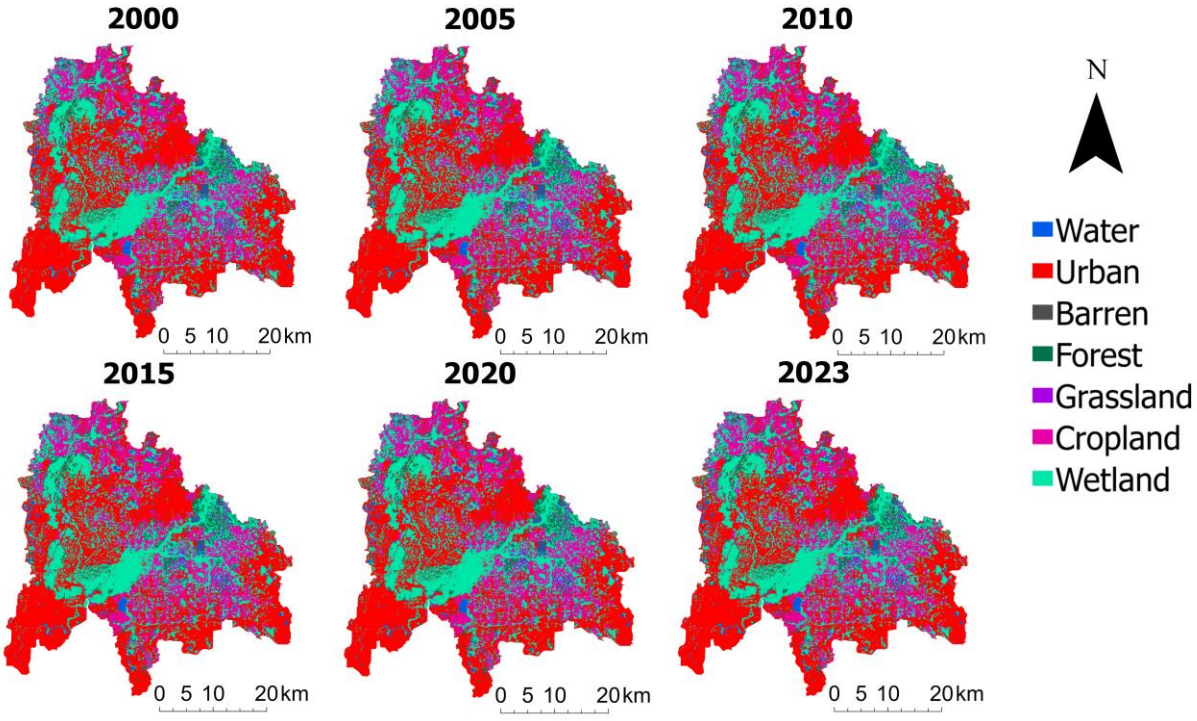

Figure 4: Spatial distribution of LULC changes from 2000 to 2023, highlighting urban expansion into cropland and wetland areas, especially in the north, central and northwest regions.

In 2000, wetlands and croplands were dominant across much of the central, north and south-eastern areas of the watershed, while forest cover was most prominent in the northern, central and eastern regions (**Figure 4**). Urban lands were largely concentrated on the southwest, northeast, and easter and southern fringes. By 2023, however, these patterns changed dramatically. The most dominant transitions occurred from cropland and wetland to urban, heavily concentrated in the northern and western sectors (**Figure 5 (a)**). The largest single transition was from cropland to urban, primarily in the northern, central and western region, with additional, patches in the south and southeast. Forest-to-urban changes tended to occur on the edges of the urban zones, most notably in the north region, where forests were cleared as towns and cities grew outward. The once-continuous wetland corridor spanning the central to eastern areas became fragmented. Wetland-to-urban conversions were most prominent in the west. Meanwhile, other transitions, such as cropland-to-wetland or cropland-to-forest, appeared but remained sparse and fragmented. Overall, these spatial patterns reflect a strong push toward urban expansion, particularly in the high-transition zone of the north, central and northwest of the watershed, with a heavy toll on agricultural and ecological landscapes.

Urban expansion was the dominant driver of change, as demonstrated by the net gains and losses in land cover types shown in **Figure 5(b)**. Urban areas experienced the highest net increase, growing by approximately 16,183 hectares. This expansion primarily occurred at the expense of cropland, wetlands, and forests, which collectively contributed to most of the land converted into urban areas.

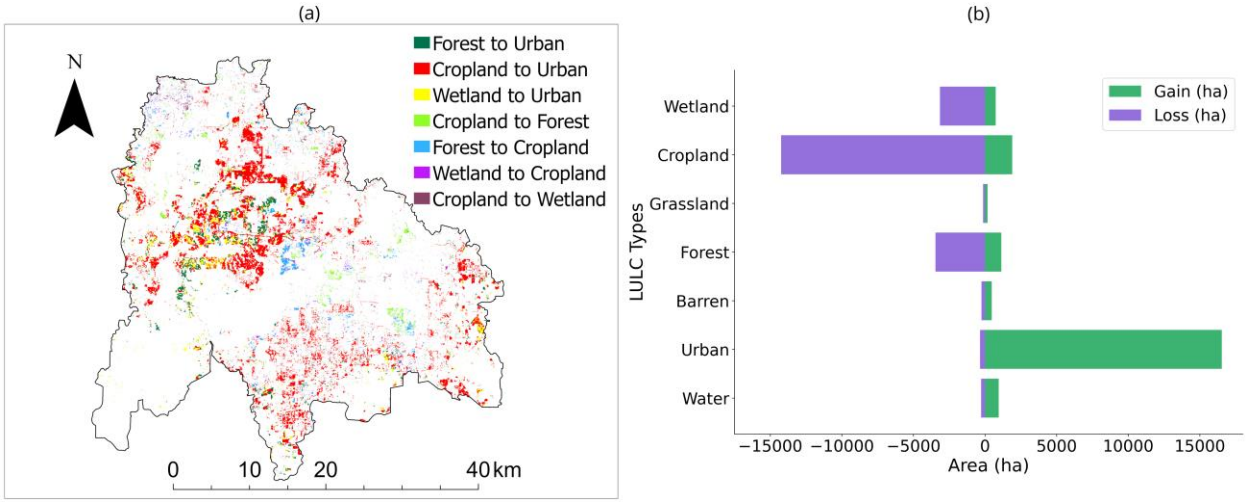

Figure 5: (a) Transition of the dominant land types **(b)** Gain and loss of lands in ha from 2000 to 2023. The figure highlights urban expansion, primarily at the expense of cropland and forest. Cropland shows the largest net loss in area, while urban land exhibits the highest net gain.

Cropland exhibited the largest net loss, decreasing by 12,355 hectares during 2000 to 2023. A substantial portion of this land was converted to urban use, reflecting the ongoing pressure of urban development on agricultural areas. Similarly, wetlands saw a decline of 2,410 hectares, with much of this area transitioning to urban land cover. Forests also contributed significantly to urban expansion, with a net loss of 2,336 hectares. Grassland and barren land exhibited minor changes in net area compared to other land types. Grassland experienced a slight increase of 28 hectares, while barren land increased by 217 hectares. Water bodies showed minimal net change, with a modest increase of 672 hectares.

3.3. ES Changes

From 2000 to 2023, ESs such as flood volume and sediment exports showed upward trends, whereas water yields and recreational visitation fluctuated. Both carbon storage and nitrogen exports experienced a steady decline. Water yields exhibited an increasing trend from 2000 to 2015, reaching a peak of $2.62 \times 10^9 m^3$, before declining to 2.05×10^9 m^3 in 2023 (**Figure 6**). Hydrological dynamics further indicated an increase in flood volume, which rose from 2.87×10^8 m^3 in 2000 to 2.93×10^8 m^3 in 2023 , while runoff retention decreased from 1.09×10^8 m^3 to 1.04×10^8 m^3 during the same period. Nutrient exports followed a declining trend, with nitrogen exports decreasing from 6.21×10^{11} kg in 2000 to 5.42×10^{11} kg in 2023.

Phosphorus exports showed a marginal reduction from 9.98×10^{11} kg to 9.69×10^{11} kg. Furthermore, sediment exports exhibited an increasing trend, rising from 3.5×10^{5} tons in 2000 to 3.83×10^{5} tons in 2023, suggesting heightened erosion risks over time. Concurrently, carbon storage declined steadily from 2.46×10^{8} tons in 2000 to 2.17×10^{8} tons in 2023, indicating a gradual reduction in stored biomass. On the other hand, visitation saw increase until the year 2011, when the number of visitations peaked at 2,711, but declined to 716 in 2017.

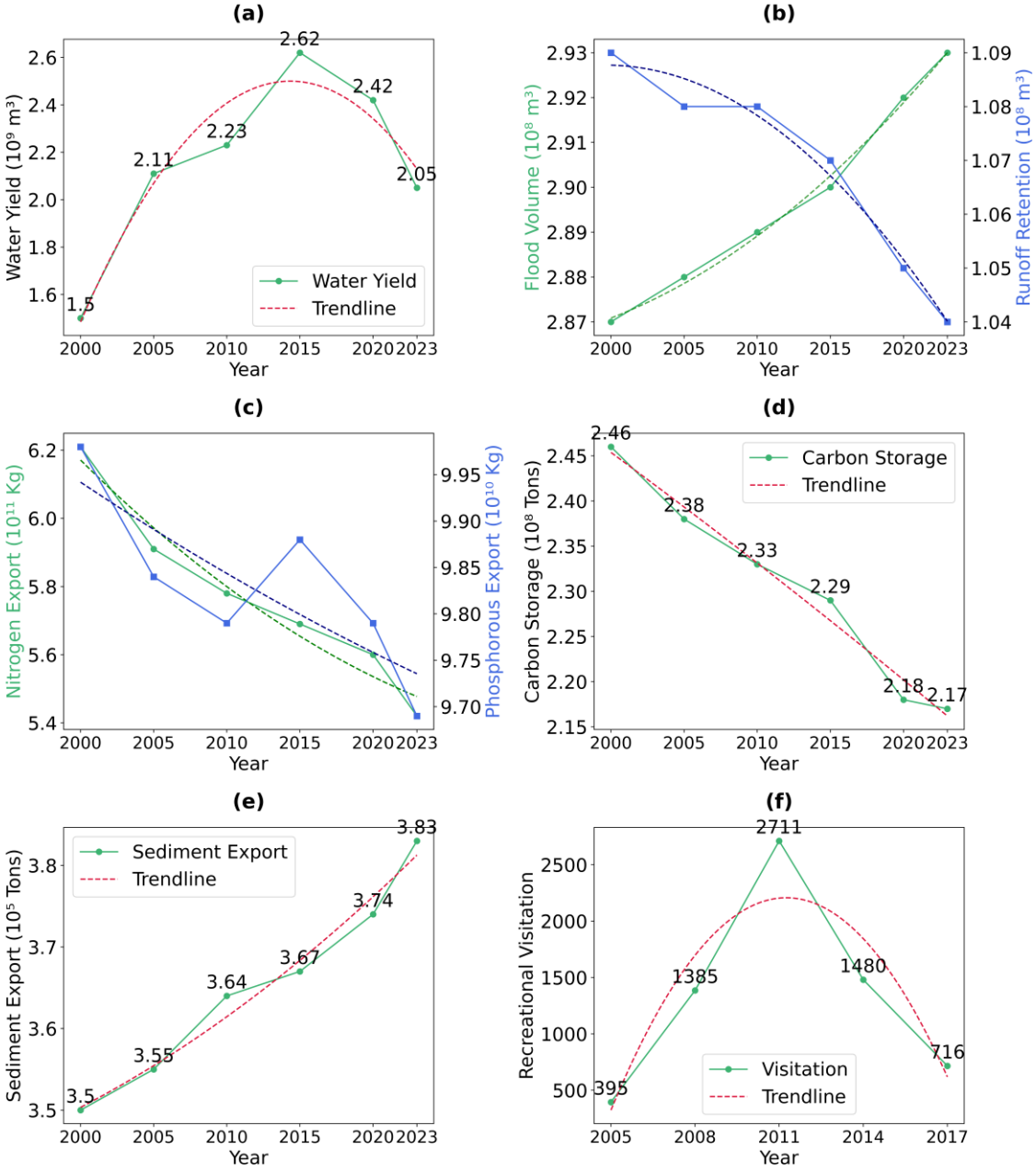

Figure 6: Changes in the ES indicators between 2000 and 2023. Flood volume and sediment export rose, while runoff retention, nitrogen and phosphorous exports, carbon storage have declined. Note that recreational visitation values are only available from 2005 to 2017, as the InVEST module generates output specifically for this time period.

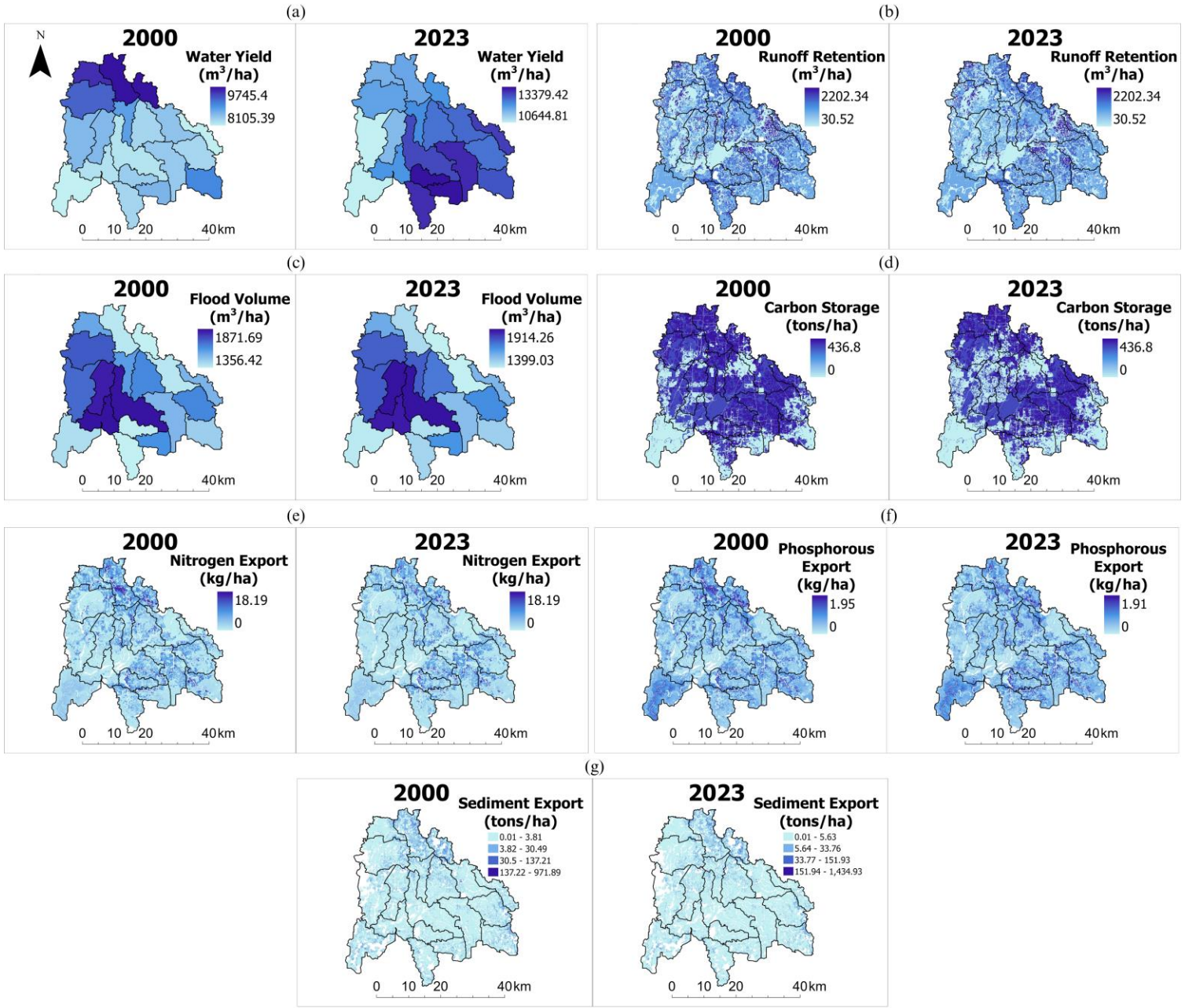

Figure 7: Spatial distribution of (a) water yield (b) runoff retention (c) flood volume and (d) carbon storage (e) nitrogen export (f) phosphorous export (g) sediment export between 2000 and 2023

Water yields demonstrated a strong spatial correlation between LULC change and hydrological outputs (**Figure 7**). Water yields increased significantly across the watershed between 2000 and 2023, with the highest concentrations observed in the southern region. Similarly, the runoff retention capacity was altered by land conversion. High-density urban areas, especially in the central and southwestern regions, showed substantial decreases in retention, a direct result of impervious surface proliferation that inhibited infiltration. Minor retention gains occurred in patches where land was restored to wetlands or forests, underlying the importance of these ecosystems in mitigating surface runoff and sustaining hydrological balance. Flood volume changes further corroborate with these findings. Zones experiencing intense urbanization, primarily central and northern areas, showed increases in flood volume, exacerbating flood risk. Carbon storage trends closely mirrored these land transitions. Areas undergoing deforestation or wetland loss, primarily in the central and northern portions of the study area, saw notable reductions in carbon stock, with some zones losing up to 436.8 tons/ha. These changes highlighted the role of forests and wetland ecosystems as critical carbon sinks and reflected how urban sprawl undermined regional carbon storage potential.

The places where cropland was converted to other land uses, especially forests, or urban areas in the central region, showed declines in nitrogen exports. A similar spatial trend was observed in phosphorus exports, with the highest increases concentrated in cropland areas, and decrease mainly in central region transitioning from cropland to urban. Sediment export patterns reflected the destabilizing effect of urban sprawl on soil and landscape integrity. Areas where forests and cropland were converted to urban land, especially in central and northern zones, saw marked increases in sediment exports, reaching up to 904.997 tons/ha.

3.4. Changes in ESV

The global coefficients were adjusted for each land type using equation (ix) and are presented in **Table 3**. For instance, the value coefficient for wetlands, one of the most valuable ecosystems, was updated from \$140,174 (2007 US\$ ha^{-1} $year^{-1}$) to \$212,593 (2024 US\$ ha^{-1} $year^{-1}$), highlighting the substantial increase in their economic significance over time.

Table 3: Global coefficients and adjusted coefficients of land types. Note that, barren area does not have any ecosystem service value. Conversely, the wetland has the largest value coefficient.

Equivalent Land Use Types	**Value Coefficient (2007 US$ ha^{-1} year $^{-1}$)**	**Adjusted Coefficient (2024 US$ ha $^{-1}$ year $^{-1}$)**
Water	12,512	18,976
Urban	6,661	10,102
Barren	0	0
Forest	5,382	8,162
Grassland	4,166	6,318
Cropland	5,567	8,443
Wetland	140,174	212,593

ESV from 2000 to 2023 highlighted a decline in total ESV, decreasing from $12,251.76 million in 2000 to $11,792,41 million in 2023, illustrating a net loss of $459.35 million (**Figure 8)**. This reduction was primarily driven by the loss of high-value ecosystems such as wetlands, forests, and croplands due to urban expansion. Wetlands, the most significant contributor to total ESV, decreased from $11,157.42 million to $10,645.03 million, reflecting a loss of $512.39 million. Similarly, croplands experienced a notable decline in ESV, dropping from $402.79 million in 2000 to $298.48 million in 2023, amounting to a loss of $104.31 million corresponding to the large-scale conversion of cropland into urban land.

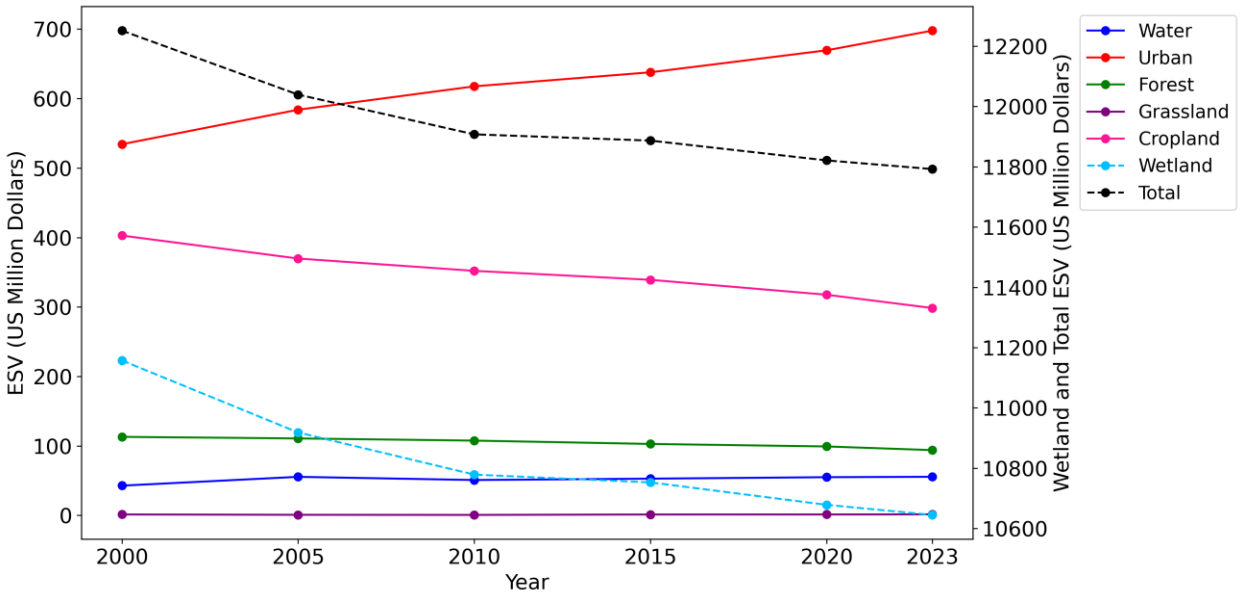

Figure 8: Changes in ESV from 2000 to 2023. While urban ESV consistently increased, total ESV declined due to losses in wetland and cropland values, reflecting a shift from high-value natural land covers to lower-value urban uses.

Urban areas, despite their lower per-hectare ESV, increased their overall contribution due to the substantial growth in urban land cover. The ESV of urban areas rose from $534.26 million in 2000 to $697.75 million in 2023, reflecting an increase of $163.49 million. This shift underscored the trade-off between urban development and ES provision. Forests, which play a crucial role in carbon sequestration and habitat provision, exhibited a decline in ESV, decreasing from $113.06 million to $94.00 million with a net loss of $19.06 million, which was consistent with the reduction in forested areas. Grassland and water bodies were smaller contributors to the total ESV and exhibited relatively minor changes. Grassland maintained a low but steady contribution, increasing slightly from $1.38 million to $1.55 million. Water bodies showed a modest increase in ESV, rising from $42.85 million to $55.60 million, potentially due to improved water resource management or slight area gains.

3.5. LULC Projections

The projected LULC changes from 2023 to 2050 illustrate a substantial transformation of the Hillsborough River Watershed, predominantly driven by urban expansion at the expense of agricultural and natural landscapes. Urban areas, which covered 40.64% of the watershed in 2023, are expected to rise steadily to 48.39% by 2050, marking a noticeable shift in land use patterns (**Figure 9)**. Spatially, this expansion is most prominent in the central, northern, southeastern, and southwestern regions, where cropland and wetlands are being converted into urban developments.

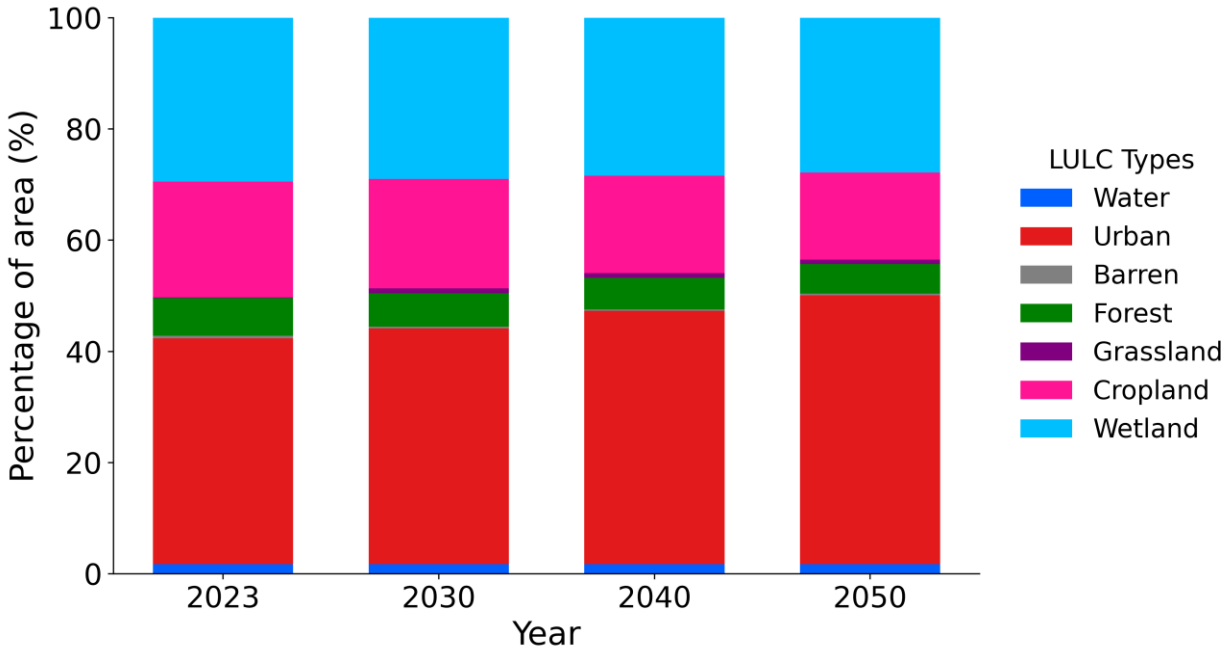

Figure 9: Future projection of LULC types (2023–2050), showing continuous urban growth at the expense of cropland, forest, and wetland. Urban land is expected to dominate by 2050, while natural (e.g., forest, wetland) and agricultural covers steadily decline.

Wetlands, historically a dominant and ecologically valuable land cover type (29.47% in 2023), are projected to decline gradually to 27.82% by 2050. This reduction is particularly noticeable in the southeastern and eastern parts of the watershed (**Figure 10**), reflecting expanding urban development into previous wetland zones. Similarly, cropland is expected to decrease from 20.80% in 2023 to 15.70% by 2050, with losses in the northern and southern regions. Forest cover is projected to diminish from 6.78% to 5.33%, while grassland is expected to increase briefly from 0.14% to 0.85% in 2030, followed by a gradual decline to 0.77% by 2050.

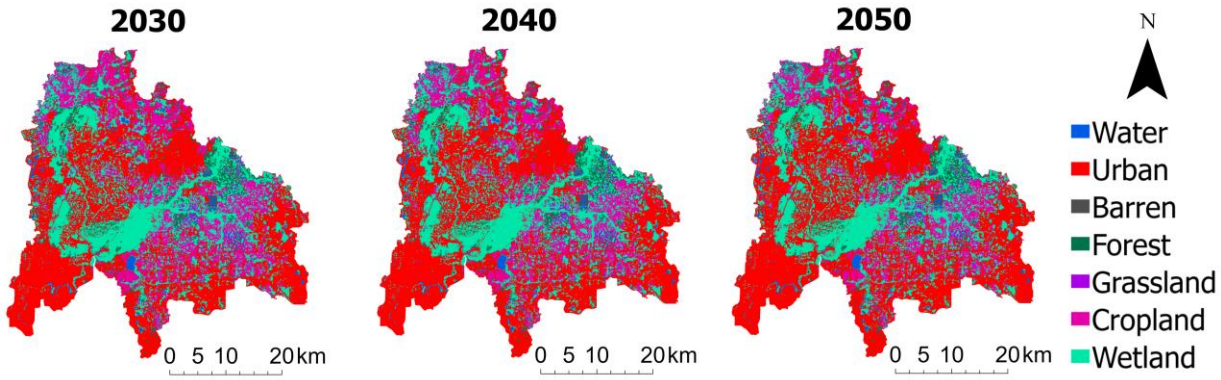

Figure 10: Spatial distribution of projected LULC for 2030, 2040, and 2050, highlighting progressive urban expansion across central, eastern and southern regions. This growth encroaches upon croplands, wetlands, and forested areas, indicating continued landscape transformation toward urban dominance.

Forest cover is also projected to diminish, dropping from 6.78% in 2030 to 5.33% in 2050, with fragmentation becoming increasingly evident, particularly in the northern areas.

3.6. Future ES and ESV

Analysis of the projected ESs for 2030, 2040, and 2050 shows changes in water resources, nutrient dynamics, carbon sequestration, and soil retention. Water yields experience a brief decline from 2.40×10^9 m³ in 2030 to 2.29×10^9 m³ in 2040, before rebounding to 2.58×10^9 m³ in 2050 (**Figure 11)**. Although the interim decrease suggests a temporary reduction in the capacity of the landscape to generate runoff, the net trend by 2050 points toward a modest overall increase in water availability. Runoff retention, however, shows a gradual decrease across the same intervals: 1.03×10^8 m³ in 2030, 1.02×10^8 m³ in 2040, and 1.01×10^8 m³ in 2050. This consistent downward trajectory indicates a potential loss in the landscape's ability to moderate surface water flows over time, reflecting diminished vegetative cover. Correspondingly, flood volume increases marginally from 2.93×10^8 m³ in 2030 to 2.94×10^8 m³ in 2040, and 2.96×10^8 m³ by 2050. The simulated increase suggests a persistent rise in flood risk, potentially driven by reduced infiltration capacity due to increased impervious land cover caused by urbanization.

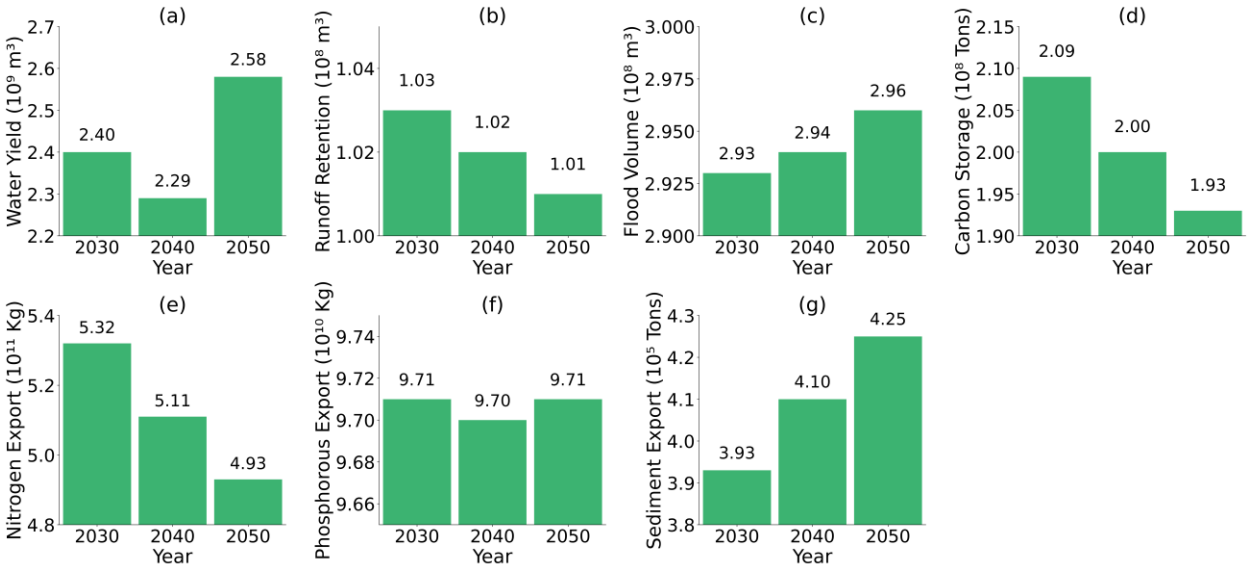

Figure 11: Projected Changes in ES Indicators (a) water yield (b) runoff retention (c) flood volume and (d) carbon storage (e) nitrogen export (f) phosphorous export (g) sediment export for 2030, 2040, and 2050. The results show an overall increase in water yield, flood volume, and sediment export over time.

In contrast, runoff retention, carbon storage, nitrogen export, and phosphorous export are expected to decline. These trends reflect the hydrological and ecological trade-offs caused by land use changes, particularly the expansion of urban areas and the reduction of vegetated land covers such as forests and wetlands.

Carbon storage decreases steadily throughout the projection period, from 2.09×10^8 tons in 2030 to 2.00×10^8 tons in 2040 and 1.93×10^8 tons in 2050, suggesting weakened sequestration potential in terrestrial ecosystems. This downward trend likely reflects ongoing pressures from land-use change, and deforestation. Meanwhile, nutrient export indicators show differing patterns. Nitrogen exports decrease from 5.32×10^{11} kg in 2030 to 5.11×10^{11} kg in 2040 and 4.93×10^{11} kg in 2050. By contrast, phosphorus exports remain essentially stable, 9.71×10^{10} kg in 2030, 9.70×10^{10} kg in 2040, and 9.71×10^{10} kg in 2050. Lastly, sediment delivery consistently increases over time, from 3.93×10^5 tons in 2030 to 4.10×10^5 tons in 2040 and 4.25×10^5 tons by 2050. This finding highlights a gradual escalation in soil erosion.

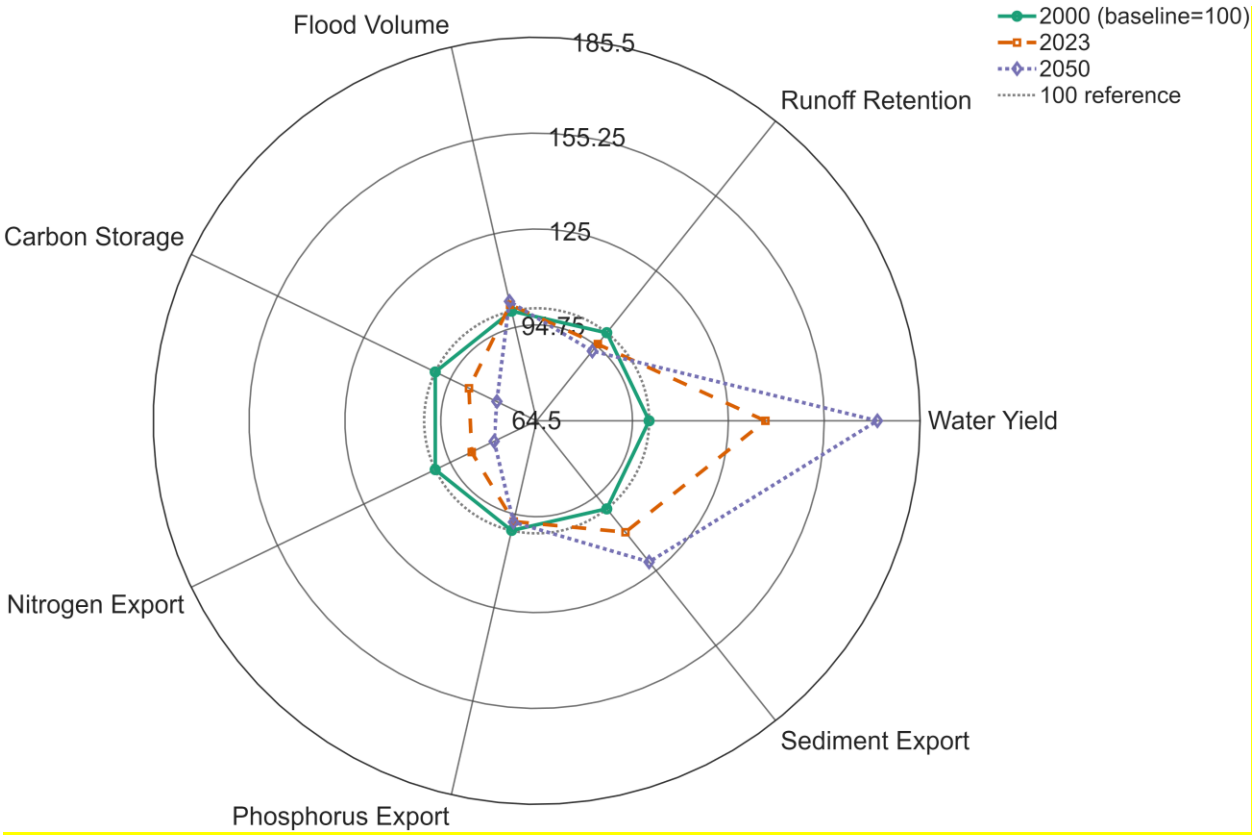

Figure 12: Relative Changes in Ecosystem Services for 2000, 2023, and 2050 (2000 Baseline = 100)

The relative changes in ecosystem service (ES) indicators for the years 2000, 2023, and 2050 are shown in **Figure 12**. The year 2000 was normalized to a baseline value of 100 for all services. Water yield showed the most pronounced increase, rising progressively in 2023 and peaking in 2050. Conversely, runoff

retention exhibited a steady decline across the study period. Flood volume changes are minimal, showing only slight increases over time. Carbon storage and nitrogen export both displayed notable decreases. Phosphorus exports show minor fluctuations, with a small net decline, whereas sediment export rose steadily, indicating increased erosion and sediment delivery in the future scenario. This visualization highlights the trade-offs between different ESs under urban expansion, with indicators like water yield increasing at the expense of key services such as carbon storage, and runoff retention.

The projection of ESV from 2023 to 2050 illustrated in **Figure 13** highlights a continuous decline in total ESV, primarily driven by reductions in high-value land cover types such as wetlands, forests, and croplands. The total ESV is expected to decrease from $11,792.41 million in 2023 to $11,228.89 million in 2050, reflecting a net loss of $563.52 million over the 27-year period. Among the LULC categories, wetlands consistently contribute the highest ESV but are projected to decline from $10,645.03 million in 2023 to $10,037.27 million in 2050, amounting to a loss of $607.76 million. Similarly, forests are estimated to decline from $93.99 million to $73.89 million, while cropland falls from $298.48 million to $224.88 million during the same period.

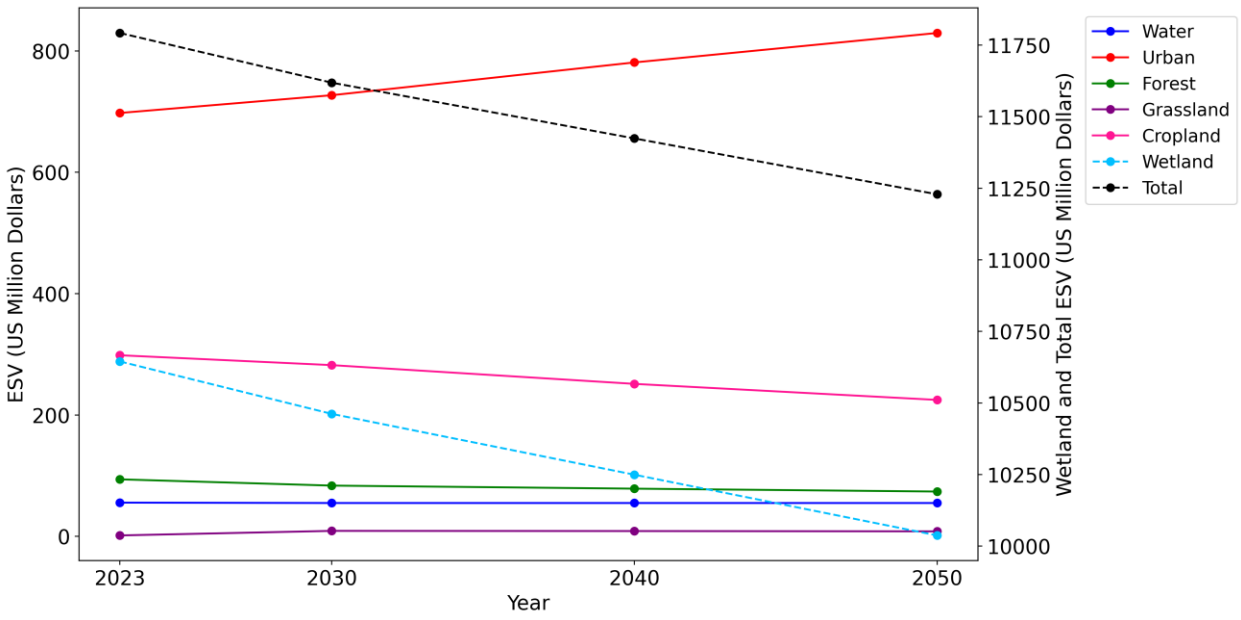

Figure 13: future ESV projection (2030, 2040, and 2050) for land use types. The total ESV is expected to decline steadily, largely due to decreases in wetland and cropland values. Wetland ESV drops sharply, contributing most to the overall loss. Cropland and forest values also show consistent declines. In contrast, urban ESV continues to rise due to land conversion, but this increase is not enough to offset the losses from natural land covers.

Conversely, the ESV of urban areas is projected to grow from $697.75 million in 2023 to $829.57 million in 2050, marking an increase of $131.82 million. This increase, however, does not compensate for the substantial ecological losses associated with the decline in natural land cover types such as forests and wetlands. Although grassland and water values show minor fluctuations, with grassland increasing from $1.55 million to $8.30 million, and water slightly decreasing from $55.60 million to $54.97 million, their contributions to the total ESV remain relatively small.

4. Discussions

4.1 Interplay between land use change and spatiotemporal ecosystem services

Changes in LULC between 2000 and 2050 alter the landscape functions, leading to noticeable impacts on the supply of ESs. Urban expansion, primarily at the expense of forests, croplands, and wetlands, has led to sharp declines in carbon storage, runoff retention, and total ESV. Carbon storage decreased from 2.46×10^8 tons in 2000 to 2.17×10^8 tons in 2023, with projections indicating a further drop to 1.93×10^8 tons by 2050. Runoff retention declined from 1.09×10^8 to 1.04×10^8 m^3 and is projected to decrease further. Previous studies have also documented declines in carbon storage and runoff retention as a consequence of urban expansion (Feng et al., 2021; Huang et al., 2024; Xiang et al., 2022; Zhang et al., 2024). Such findings align with the well-established understanding that urbanization disrupts key regulating services by reducing wetlands, fragmenting natural habitats, and expanding impervious surface areas (Cao et al., 2021; Ouyang et al., 2021; Pham & Lin, 2023b).

Water yield exhibited a non-linear pattern, peaking around 2020 before declining, likely reflecting both land cover change and interannual precipitation variability. Notably, the 2023 low coincides with a below-average annual rainfall of about 44.8 inches compared to 56.3 inches in 2015 and 52.5 inches in 2020 (**Figure S1**). Projections of water yields indicate a moderate rebound by 2050, consistent with trends in urbanizing watersheds (Kumar et al., 2018; C. Li et al., 2020; R. Zhou et al., 2025). This slight rebound can be explained by the combination of higher projected precipitation and reduced evapotranspiration due to urban expansion. Nutrient exports showed a declining trend, with nitrogen exports decreasing from 6.21×10^{11} to 5.42×10^{11} kg. This is largely due to the reduction in agricultural land as many croplands were converted into urban and forested areas. Newer urban areas often use less fertilizer than cropland, while forests are associated with deeper root systems and more organic-rich soils that absorb and retain nitrogen. Conversely, sediment exports increased steadily, reaching 4.25×10^5 tons by 2050. Urban expansion intensifies surface runoff and concentrated sediment transport through impervious surfaces and drainage networks, enhancing sediment connectivity and delivery to streams (McVey et al., 2023; Zarnaghsh & Husic, 2021; M. Zhou et al., 2019). Furthermore, increased sediment exports and flood volume in high-transition zones (central, north, and northwest) highlighted hydrological impacts.

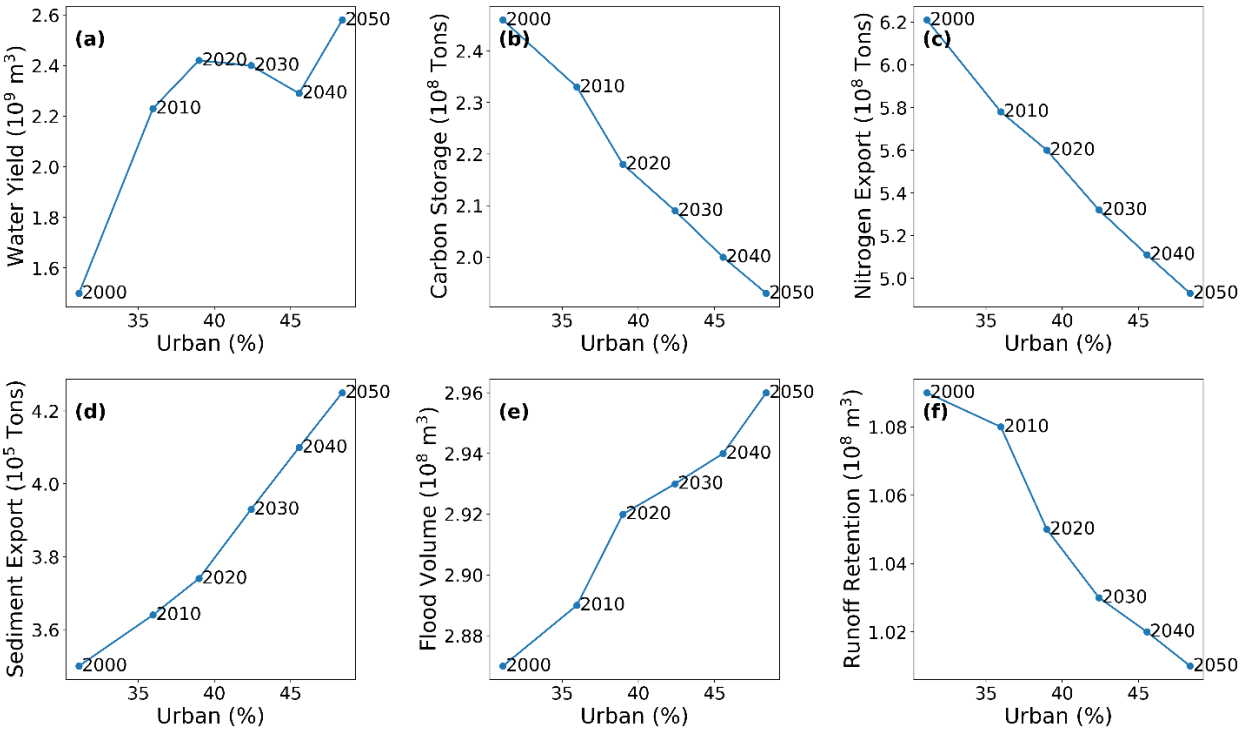

Figure 14: the relationships between urban land cover percentage and ecosystem service indicators from 2000 to 2050. As urbanization increases, (b) carbon storage, (c) nitrogen export, and (f) runoff retention all shows consistent declines, highlighting the negative ecological impacts of urban growth. (d) Sediment export and (e) flood volume, however, increase steadily with urban expansion, indicating greater erosion and runoff. (a) Water yield exhibits a non-linear pattern.

Urban expansion is one of the dominant forces behind ES degradation in the study area shown in **Figure 14**. Wetlands and forests that were associated with the highest per-hectare ESVs saw the largest area reductions, contributing to a total ESV loss of over $1 billion between 2000 and 2050. This pattern supports previous findings that even small losses in wetland area can result in ecological and economic impacts (Long et al., 2022b; Song et al., 2021).

4.2 Policy implications and strategies for enhancing ES recognition, valuation, and resilience

The decline in ecosystem services highlights the urgent need for policies that protect high-value ecosystems such as wetlands and forests from further conversion. These areas deliver critical regulating services, including carbon sequestration, water retention, and nutrient regulation, that underpin local climate resilience and water security. Protecting them aligns directly with SDGs 6 (Clean Water and Sanitation), 11 (Sustainable Cities and Communities), 13 (Climate Action), and 15 (Life on Land). Urban expansion should

be guided by land-use planning frameworks that integrate ecosystem service valuation into zoning and permitting processes.

To mitigate further degradation, targeted ecological restoration is urgently needed, especially in high-transition zones. ES loss and high transition zones identified in this study can be prioritized for restoration, ecological buffer creation, and green infrastructure investments. For example, wetland buffer zones, reforestation corridors, and low-impact development (LID) designs can help mitigate flood risk, reduce sediment loads, and maintain biodiversity (Goyette et al., 2023; Serra-Llobet et al., 2022; Radcliffe, 2019). Future development should be guided by ecological zoning, and the careful conversion of low-value barren land instead of high-value natural ecosystems. Moreover, integrating recreational green spaces into urban design could help sustain cultural services amid continued urbanization (Udayasoorian & Ramalingam, 2025). Strategic land management and planning will be crucial for balancing urban growth with long-term ecological sustainability.

Recognizing the socio-economic dimension is equally important. Increased flood risk and reduced carbon storage from urban expansion can damage infrastructure, disrupt livelihoods, and pose safety hazards for residents (Dodman et al., 2022). Such impacts often disproportionately affect vulnerable populations, highlighting the need for equity-focused adaptation strategies (Foster et al., 2024). By combining findings from this study with demographic and socio-economic data, local governments can identify high-risk areas and prioritize investments that reduce both physical and social vulnerability. Governance challenges, such as fragmented decision-making, limited enforcement capacity, and competing stakeholder priorities can hinder implementation (Crosby, 1996). Overcoming these requires coordinated planning between municipalities, water management districts, and environmental agencies. Cross-jurisdictional agreements, incentives for private land conservation, and active community engagement can strengthen governance effectiveness. Sustainable urban futures depend on policies that elevate ecosystem service preservation alongside economic development, safeguarding the resilience of both human and natural systems.

4. Conclusions

This study demonstrates that historical and projected LULC changes between 2000 and 2050 will substantially alter ES provision in the Hillsborough River watershed. Urban expansion, primarily replacing forests, wetlands, and croplands, drives decline in key regulating and supporting services, including carbon storage, runoff retention, and nitrogen retention. Total ESV is projected to fall by more than $1 billion over the study period. These losses are accompanied by increased sediment exports and higher flood volumes, indicating heightened hydrological risks. Water yield trends show a non-linear pattern, influenced by both land cover transitions and rainfall variability.

The findings highlight three key takeaways:

1. Urban growth patterns matter - targeting development away from high-ESV landscapes is critical to minimize ecological and economic losses.
2. Nature-based solutions are essential - conserving wetlands, restoring forest buffers, and implementing green infrastructure may enhance resilience and reduce flood risk.
3. Integrated planning can align ecology and economy - ecological zoning and strategic land-use planning may balance urban expansion with long-term sustainability.

While the integrated use of InVEST and TerrSet's LCM provides valuable long-term projections, the study acknowledges certain limitations. Several InVEST modules simplify ecological processes. For instance, the water yield model omits sub-annual variability and subsurface flows, the carbon model assumes static carbon pools, and sediment modeling excludes gully and streambank erosion. A comprehensive calibration and validation of the result was not possible due to limited catchment level observational data collected at consistent temporal and spatial scales. Given these limitations, the results should be interpreted as indicative trends rather than precise values, reflecting uncertainties in model inputs and assumptions. Additionally, the analysis of ESV relied on global literature-derived coefficients also due to lack of local data. Future work should use higher-resolution socio-economic and climate data, adopt dynamic process-based models, and expand ES coverage to include biodiversity, food production, and climate regulation to fully capture the watershed's ecological and economic value.

Acknowledgement

The research was supported by the Federal Finance Assistant Award of Domestic Grant 24-DG-11083150-705 to Florida A&M University by USDA Forest Service.

Conflicts of Interest

On behalf of all authors, the corresponding author states that there is no conflict of interest.

5. References:

Aghaloo, K., & Sharifi, A. (2025). Balancing priorities for a sustainable future in cities: Land use change and urban ecosystem service dynamics. *Journal of Environmental Management, 382*, 125460. https://doi.org/10.1016/j.jenvman.2025.125460

Biedemariam, M., Birhane, E., Demissie, B., Tadesse, T., Gebresamuel, G., & Habtu, S. (2022). Ecosystem Service Values as Related to Land Use and Land Cover Changes in Ethiopia: A Review. *Land*, *11*(12). https://doi.org/10.3390/LAND11122212

Cao, Y., Kong, L., Zhang, L., & Ouyang, Z. (2021). The balance between economic development and ecosystem service value in the process of land urbanization: A case study of China's land urbanization from 2000 to 2015. *Land Use Policy*, *108*. https://doi.org/10.1016/J.LANDUSEPOL.2021.105536

Costanza, R., de Groot, R., Sutton, P., van der Ploeg, S., Anderson, S. J., Kubiszewski, I., Farber, S., & Turner, R. K. (2014). Changes in the global value of ecosystem services. *Global Environmental Change*, *26*(1), 152–158. https://doi.org/10.1016/J.GLOENVCHA.2014.04.002

Crosby, B. L. (1996). Policy implementation: The organizational challenge. World Development, 24(9), 1403–1415. https://doi.org/10.1016/0305-750X(96)00050-2

Dodman, D., Hayward, B., Pelling, M., Castan Broto, V., Chow, W., Chu, E., Dawson, R., Khirfan, L., McPhearson, T., Prakash, A., Zheng, Y., & Ziervogel, G. (2022). Cities, settlements and key infrastructure. In H.-O. Pörtner, D. C. Roberts, M. Tignor, E. S. Poloczanska, K. Mintenbeck, A. Alegría, M. Craig, S. Langsdorf, S. Löschke, V. Möller, A. Okem, & B. Rama (Eds.), Climate Change 2022: Impacts, Adaptation and Vulnerability. Contribution of Working Group II to the Sixth Assessment Report of the Intergovernmental Panel on Climate Change (pp. 907–1040). Cambridge University Press. https://doi.org/10.1017/9781009325844.008

Fang, Z., Ding, T., Chen, J., Xue, S., Zhou, Q., Wang, Y., Wang, Y., Huang, Z., & Yang, S. (2022). Impacts of land use/land cover changes on ecosystem services in ecologically fragile regions. *Science of The Total Environment*, *831*, 154967. https://doi.org/10.1016/J.SCITOTENV.2022.154967

Feng, B., Zhang, Y., & Bourke, R. (2021). Urbanization impacts on flood risks based on urban growth data and coupled flood models. *Natural Hazards*, *106*(1), 613–627. https://doi.org/10.1007/S11069-020-04480-0

Forootan, E. (2023). GIS-based slope-adjusted curve number methods for runoff estimation. *Environmental Monitoring and Assessment*, *195*(4), 1–18. https://doi.org/10.1007/S10661-023-11039-6/TABLES/6

Foster, S. R., Baptista, A., Nguyen, K. H., Tchen, J., Tedesco, M., & Leichenko, R. (2024). NPCC4: Advancing climate justice in climate adaptation strategies for New York City. Annals of the New York Academy of Sciences, 1539(1), 77–126. https://doi.org/10.1111/nyas.15148

Gan, G., Liu, Y., & Sun, G. (2021). Understanding interactions among climate, water, and vegetation with the Budyko framework. *Earth-Science Reviews*, *212*. https://doi.org/10.1016/J.EARSCIREV.2020.103451

Gomes, E., Inácio, M., Bogdzevič, K., Kalinauskas, M., Karnauskaitė, D., & Pereira, P. (2021). Future land-use changes and its impacts on terrestrial ecosystem services: A review. *Science of The Total Environment*, *781*, 146716. https://doi.org/10.1016/J.SCITOTENV.2021.146716

Goyette, J. O., Savary, S., Blanchette, M., & others. (2023). Setting targets for wetland restoration to mitigate climate change effects on watershed hydrology. Environmental Management, 71(2), 365–378. https://doi.org/10.1007/s00267-022-01763-z

Guo, M., Ma, S., Wang, L. J., & Lin, C. (2021). Impacts of future climate change and different management scenarios on water-related ecosystem services: A case study in the Jianghuai ecological economic Zone, China. *Ecological Indicators*, *127*. https://doi.org/10.1016/j.ecolind.2021.107732

Huang, S., Gan, Y., Chen, N., Wang, C., Zhang, X., Li, C., & Horton, D. E. (2024). Urbanization enhances channel and surface runoff: A quantitative analysis using both physical and empirical models over the Yangtze River basin. *Journal of Hydrology*, *635*. https://doi.org/10.1016/J.JHYDROL.2024.131194

Ismaili Alaoui, H., Chemchaoui, A., El Asri, B., Ghazi, S., Brhadda, N., & Ziri, R. (2023). Modeling predictive changes of carbon storage using invest model in the Beht watershed (Morocco). *Modeling Earth Systems and Environment*, *9*(4), 4313–4322. https://doi.org/10.1007/s40808-023-01697-3

Jian, Z., Sun, Y., Wang, F., Zhou, C., Pan, F., Meng, W., & Sui, M. (2024). Soil conservation ecosystem service supply-demand and multi scenario simulation in the Loess Plateau, China. *Global Ecology and Conservation*, *49*, e02796. https://doi.org/10.1016/J.GECCO.2023.E02796

Jiang, H., Wu, W., Wang, J., Yang, W., Gao, Y., Duan, Y., Ma, G., Wu, C., & Shao, J. (2021). Mapping global value of terrestrial ecosystem services by countries. *Ecosystem Services*, *52*, 101361. https://doi.org/10.1016/J.ECOSER.2021.101361

Kumar, S., Moglen, G. E., Godrej, A. N., Grizzard, T. J., & Post, H. E. (2018). Trends in Water Yield under Climate Change and Urbanization in the US Mid-Atlantic Region. *Journal of Water Resources Planning and Management*, *144*(8). https://doi.org/10.1061/(asce)wr.1943-5452.0000937

Lal, R., Monger, C., Nave, L., & Smith, P. (2021). The role of soil in regulation of climate. *Philosophical Transactions of the Royal Society B: Biological Sciences*, *376*(1834). https://doi.org/10.1098/RSTB.2021.0084

Li, C., Sun, G., Caldwell, P. V., Cohen, E., Fang, Y., Zhang, Y., Oudin, L., Sanchez, G. M., & Meentemeyer, R. K. (2020). Impacts of urbanization on watershed water balances across the conterminous United States. *Water Resources Research*, *56*(7), 1–19. https://doi.org/10.1029/2019WR026574

Li, L., Tang, H., Lei, J., & Song, X. (2022). Spatial autocorrelation in land use type and ecosystem service value in Hainan Tropical Rain Forest National Park. *Ecological Indicators*, *137*. https://doi.org/10.1016/J.ECOLIND.2022.108727

Li, X., Huang, C., Jin, H., Han, Y., Kang, S., Liu, J., Cai, H., Hu, T., Yang, G., Yu, H., & Sun, L. (2022). Spatio-Temporal Patterns of Carbon Storage Derived Using the InVEST Model in Heilongjiang Province, Northeast China. *Frontiers in Earth Science*, *10*. https://doi.org/10.3389/feart.2022.846456

Li, Y., Liu, W., Feng, Q., Zhu, M., Yang, L., Zhang, J., & Yin, X. (2023). The role of land use change in affecting ecosystem services and the ecological security pattern of the Hexi Regions, Northwest China. *Science of the Total Environment*, *855*. https://doi.org/10.1016/J.SCITOTENV.2022.158940

Liu, L., & Wu, J. (2022). Scenario analysis in urban ecosystem services research: Progress, prospects, and implications for urban planning and management. *Landscape and Urban Planning*, *224*. https://doi.org/10.1016/J.LANDURBPLAN.2022.104433

Long, X., Lin, H., An, X., Chen, S., Qi, S., & Zhang, M. (2022a). Evaluation and analysis of ecosystem service value based on land use/cover change in Dongting Lake wetland. *Ecological Indicators*, *136*. https://doi.org/10.1016/J.ECOLIND.2022.108619

Long, X., Lin, H., An, X., Chen, S., Qi, S., & Zhang, M. (2022b). Evaluation and analysis of ecosystem service value based on land use/cover change in Dongting Lake wetland. *Ecological Indicators*, *136*. https://doi.org/10.1016/J.ECOLIND.2022.108619

Lu, Y., Yang, J., Peng, M., Li, T., Wen, D., & Huang, X. (2022). Monitoring ecosystem services in the Guangdong-Hong Kong-Macao Greater Bay Area based on multi-temporal deep learning. *Science of the Total Environment*, *822*. https://doi.org/10.1016/j.scitotenv.2022.153662

McVey, I., Michalek, A., Mahoney, T., & Husic, A. (2023). Urbanization as a limiter and catalyst of watershed-scale sediment transport: Insights from probabilistic connectivity modeling. *Science of the Total Environment*, *894*. https://doi.org/10.1016/j.scitotenv.2023.165093

Mohammadyari, F., Zarandian, A., Mirsanjari, M. M., Suziedelyte Visockiene, J., & Tumeliene, E. (2023). Modelling Impact of Urban Expansion on Ecosystem Services: A Scenario-Based Approach in a Mixed Natural/Urbanised Landscape. *Land*, *12*(2). https://doi.org/10.3390/land12020291

Munna, G. M., Alam, M. J. Bin, Uddin, M. M., Islam, N., Orthee, A. A., & Hasan, K. (2021). Runoff prediction of Surma basin by curve number (CN) method using ARC-GIS and HEC-RAS. *Environmental and Sustainability Indicators*, *11*, 100129. https://doi.org/10.1016/J.INDIC.2021.100129

Nahib, I., Ambarwulan, W., Rahadiati, A., Munajati, S. L., Prihanto, Y., Suryanta, J., Turmudi, T., & Nuswantoro, A. C. (2021). Assessment of the impacts of climate and LULC changes on the water yield in the citarum River Basin, West Java Province, Indonesia. *Sustainability (Switzerland)*, *13*(7). https://doi.org/10.3390/su13073919

Ouyang, X., Tang, L., Wei, X., & Li, Y. (2021). Spatial interaction between urbanization and ecosystem services in Chinese urban agglomerations. *Land Use Policy*, *109*, 105587. https://doi.org/10.1016/J.LANDUSEPOL.2021.105587

Petsch, D. K., Cionek, V. de M., Thomaz, S. M., & dos Santos, N. C. L. (2023). Ecosystem services provided by river-floodplain ecosystems. *Hydrobiologia*, *850*(12–13), 2563–2584. https://doi.org/10.1007/S10750-022-04916-7

Pham, K. T., & Lin, T. H. (2023a). Effects of urbanisation on ecosystem service values: A case study of Nha Trang, Vietnam. *Land Use Policy*, *128*. https://doi.org/10.1016/J.LANDUSEPOL.2023.106599

Pham, K. T., & Lin, T. H. (2023b). Effects of urbanisation on ecosystem service values: A case study of Nha Trang, Vietnam. *Land Use Policy*, *128*. https://doi.org/10.1016/J.LANDUSEPOL.2023.106599

Publications - IPCC-TFI. (n.d.). Retrieved February 27, 2025, from https://www.ipcc-nggip.iges.or.jp/public/2006gl/vol4.html

Radcliffe, J. C. (2019). History of water sensitive urban design/low impact development adoption in Australia and internationally. In A. K. Sharma, T. Gardner, & D. Begbie (Eds.), Approaches to water sensitive urban design (pp. 1–24). Woodhead Publishing. https://doi.org/10.1016/B978-0-12-812843-5.00001-0

Redhead, J. W., May, L., Oliver, T. H., Hamel, P., Sharp, R., & Bullock, J. M. (2018). National scale evaluation of the InVEST nutrient retention model in the United Kingdom. *Science of The Total Environment*, *610–611*, 666–677. https://doi.org/10.1016/J.SCITOTENV.2017.08.092

Schirpke, U., Tasser, E., Borsky, S., Braun, M., Eitzinger, J., Gaube, V., Getzner, M., Glatzel, S., Gschwantner, T., Kirchner, M., Leitinger, G., Mehdi-Schulz, B., Mitter, H., Scheifinger, H., Thaler, S., Thom, D., & Thaler, T. (2023). Past and future impacts of land-use changes on ecosystem services in Austria. *Journal of Environmental Management*, *345*. https://doi.org/10.1016/J.JENVMAN.2023.118728

Serra-Llobet, A., Jähnig, S. C., Geist, J., Kondolf, G. M., Damm, C., Scholz, M., Lund, J., Opperman, J. J., Yarnell, S. M., Pawley, A., Shader, E., Cain, J., Zingraff-Hamed, A., Grantham, T. E., Eisenstein, W., & Schmitt, R. (2022). Restoring rivers and floodplains for habitat and flood risk reduction: Experiences in multi-benefit floodplain management from California and Germany. Frontiers in Environmental Science, 9, 778568. https://doi.org/10.3389/fenvs.2021.778568

Smith, J. E., Heath, L. S., Skog, K. E., & Birdsey, R. A. (2006). Methods for calculating forest ecosystem and harvested carbon with standard estimates for forest types of the United States. *Gen. Tech. Rep. NE-343. Newtown Square, PA: U.S. Department of Agriculture, Forest Service, Northeastern Research Station. 216 p.*, *343*. https://doi.org/10.2737/NE-GTR-343

Song, F., Su, F., Mi, C., & Sun, D. (2021). Analysis of driving forces on wetland ecosystem services value change: A case in Northeast China. *Science of the Total Environment*, *751*. https://doi.org/10.1016/J.SCITOTENV.2020.141778

Sun, L., Yu, H., Sun, M., & Wang, Y. (2023). Coupled impacts of climate and land use changes on regional ecosystem services. *Journal of Environmental Management*, *326*. https://doi.org/10.1016/j.jenvman.2022.116753

Tilman, D., Hill, J., & Lehman, C. (2006). Carbon-negative biofuels from low-input high-diversity grassland biomass. *Science*, *314*(5805), 1598–1600. https://doi.org/10.1126/SCIENCE.1133306/SUPPL_FILE/TILMAN.SOM.REV1.PDF

Torres, A. V., Tiwari, C., & Atkinson, S. F. (2021). Progress in ecosystem services research: A guide for scholars and practitioners. *Ecosystem Services*, *49*, 101267. https://doi.org/10.1016/J.ECOSER.2021.101267

Udayasoorian, K. P., & Ramalingam, S. (2025). Enhancing sustainable urban planning to mitigate urban heat island effects through residential greening. Sustainable Cities and Society, 129, 106512. https://doi.org/10.1016/j.scs.2025.106512

Wang, C., Wang, S., Fu, B., & Zhang, L. (2016). Advances in hydrological modelling with the Budyko framework: A review. *Progress in Physical Geography*, *40*(3), 409–430. https://doi.org/10.1177/0309133315620997

Wang, R., Zhao, J., Chen, G., Lin, Y., Yang, A., & Cheng, J. (2022). Coupling PLUS–InVEST Model for Ecosystem Service Research in Yunnan Province, China. *Sustainability 2023, Vol. 15, Page 271*, *15*(1), 271. https://doi.org/10.3390/SU15010271

Xiang, S., Wang, Y., Deng, H., Yang, C., Wang, Z., & Gao, M. (2022). Response and multi-scenario prediction of carbon storage to land use/cover change in the main urban area of Chongqing, China. *Ecological Indicators*, *142*. https://doi.org/10.1016/J.ECOLIND.2022.109205

Xiao, J., Song, F., Su, F., Shi, Z., & Song, S. (2023). Quantifying the independent contributions of climate and land use change to ecosystem services. *Ecological Indicators*, *153*. https://doi.org/10.1016/j.ecolind.2023.110411

Zarandian, A., Mohammadyari, F., Mirsanjari, M. M., & Visockiene, J. S. (2023). Scenario modeling to predict changes in land use/cover using Land Change Modeler and InVEST model: a case study of Karaj Metropolis, Iran. *Environmental Monitoring and Assessment*, *195*(2), 1–22. https://doi.org/10.1007/S10661-022-10740-2/FIGURES/7

Zarnaghsh, A., & Husic, A. (2021). Degree of Anthropogenic Land Disturbance Controls Fluvial Sediment Hysteresis. *Environmental Science and Technology*, *55*(20), 13737–13748. https://doi.org/10.1021/acs.est.1c00740

Zhang, Y., Liao, X., & Sun, D. (2024). A Coupled InVEST-PLUS Model for the Spatiotemporal Evolution of Ecosystem Carbon Storage and Multi-Scenario Prediction Analysis. *Land*, *13*(4). https://doi.org/10.3390/land13040509

Zhou, M., Deng, J., Lin, Y., Belete, M., Wang, K., Comber, A., Huang, L., & Gan, M. (2019). Identifying the effects of land use change on sediment export: Integrating sediment source and sediment delivery in the

Qiantang River Basin, China. *Science of the Total Environment*, *686*, 38–49. https://doi.org/10.1016/j.scitotenv.2019.05.336

Zhou, R., Zhou, Y., Zhu, W., Feng, L., & Liu, L. (2025). Projecting Water Yield Amidst Rapid Urbanization: A Case Study of the Taihu Lake Basin. *Land*, *14*(1). https://doi.org/10.3390/land14010149

Zhu, K., Cheng, Y., Zhou, Q., & Azadi, H. (2024). Understanding future water-carbon-land coupled systems in the era of COP 27: The case of the Hanjiang River Basin, China. *Journal of Cleaner Production, 479*, 144054. https://doi.org/10.1016/j.jclepro.2024.144054

Supporting Information for

Impact of Land Use Land Cover Changes on Ecosystem Services: A Multi-Module InVEST-LCM Analysis

Fahad Hasan [a]* 0009-0009-7824-5538, Yashar Makhtoumi [b] 0000-0002-0305-6849, Gang Chen [a] 0000-0002-6476-7812

[a] Department of Civil and Environmental Engineering, Florida State University, Tallahassee, FL 32310, USA a
[b] Center for Sustainability and the Global Environment, Nelson Institute for Environmental Studies, University of Wisconsin-Madison, Madison, WI 53726, USA b

* Correspondence: Fahad Hasan, fh23b@fsu.edu

Contents of this file

Introduction

This Supplementary information provides extended data and spatial insights that support the main findings of the manuscript. Included are definitions of technical terms that are used in the manuscript, additional figures that illustrate precipitation patterns, spatial projections of key ESs under future land use, and the detailed determination of the Kappa coefficient for LULC classification accuracy assessment. These materials aim to enhance transparency, reproducibility, and interpretation of the modeling framework and its outputs.

Definitions of Technical Terms

Annual water yield: The total amount of water (from rainfall and other sources) that flows out of a watershed into rivers and streams over one year.

Carbon storage: The amount of carbon kept in forests, soils, and other ecosystems instead of being released into the atmosphere as carbon dioxide.

Runoff retention: The ability of the land to hold back rainwater and reduce flooding, rather than letting it flow quickly into rivers.

Sediment export: The movement of soil and sand from land into rivers or lakes, often increased by deforestation or urbanization.

Nutrient export: The amount of nutrients (like nitrogen or phosphorus) that leave farmland or other areas and flow into rivers, potentially causing water pollution.

Ecosystem service value (ESV): The economic worth of benefits that nature provides to people, such as clean water, flood protection, or carbon storage.

Transition zones: Areas where land use is changing rapidly (e.g., from forest to urban).

Low-impact development (LID): Urban design techniques (like green roofs or rain gardens) that reduce flooding and pollution.

Barren land: Areas with little or no vegetation, such as exposed soil or rocks.

Carbon sequestration: The process of capturing and storing carbon dioxide in plants, soils, or other ecosystems.

Nutrient regulation: The natural ability of ecosystems (like wetlands or forests) to absorb and filter nutrients, preventing water pollution.

Buffer zones: Strips of land (often with vegetation) set aside between natural areas and human activity to reduce environmental damage.

Text S1.

The bar chart in **Figure S1** illustrates annual precipitation for the Hillsborough River Watershed from 2000 to 2050. Precipitation showed a marked increase from 802.64 mm in 2000 to over 1400 mm by 2010 and

2015. After a slight decrease to 1333.5 mm in 2020 and further down to 1137.92 mm in 2023, rainfall is projected to rise again, reaching 1516.85 mm by 2050. The years 2000 and 2023 recorded the lowest rainfall, while 2050 is projected to be the wettest year in the dataset.

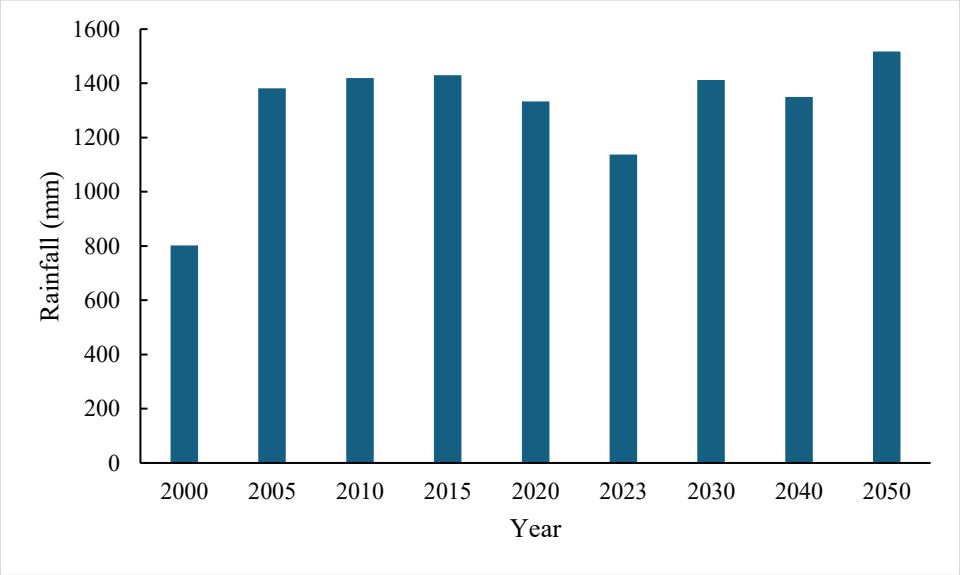

Figure S1. Annual rainfall estimates for Hillsborough River Watershed (https://hillsborough.wateratlas.usf.edu/rainfall/estimates/)**.** The chart highlights interannual variability, with minimum rainfall in 2000 (802.64 mm) and 2023 (1137.92 mm), and a projected peak in 2050 (1516.85 mm).

Text S2.

Based on the spatial projections of ecosystem services for 2030, 2040, and 2050 (**Figure S2**), notable patterns emerge. Water yield is consistently higher in the northern and northwestern regions for all three years. Similarly, flood volume follows this pattern, with central and western regions contributing the most. Runoff retention, on the other hand, remains highest in areas with intact wetlands and forested patches, primarily located in scattered zones across the eastern and southern watershed. However, retention values show a decreasing trend from 2030 to 2050, particularly in areas undergoing urban expansion. Carbon storage exhibits a more widespread decline, especially in the central and southern regions. Nitrogen and phosphorous export patterns are denser in the northern and southern regions, reflecting the cropland-dominated regions. Sediment export shows higher values along riparian corridors and disturbed zones, with a consistent increase by 2050.

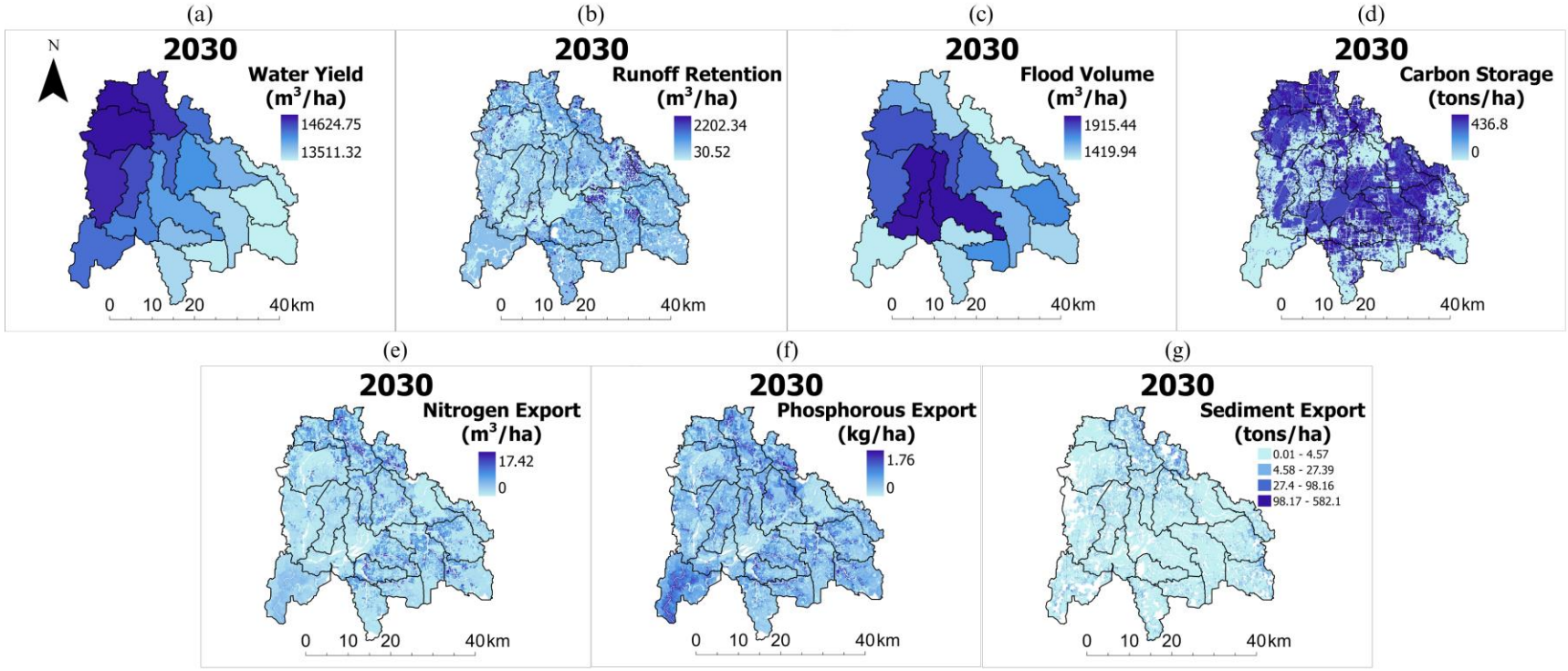
(a)
(b)
(c)
(d)
N
2030
Water Yield
(m³/ha)
14624.75
13511.32
2030
Runoff Retention
(m³/ha)
2202.34
30.52
2030
Flood Volume
(m³/ha)
1915.44
1419.94
2030
Carbon Storage
(tons/ha)
436.8
0
0 10 20 40km
(e)
(f)
(g)
2030
Nitrogen Export
(m³/ha)
17.42
0
2030
Phosphorous Export
(kg/ha)
1.76
0
2030
Sediment Export
(tons/ha)
0.01 - 4.57
4.58 - 27.39
27.4 - 98.16
98.17 - 582.1

(cont.)

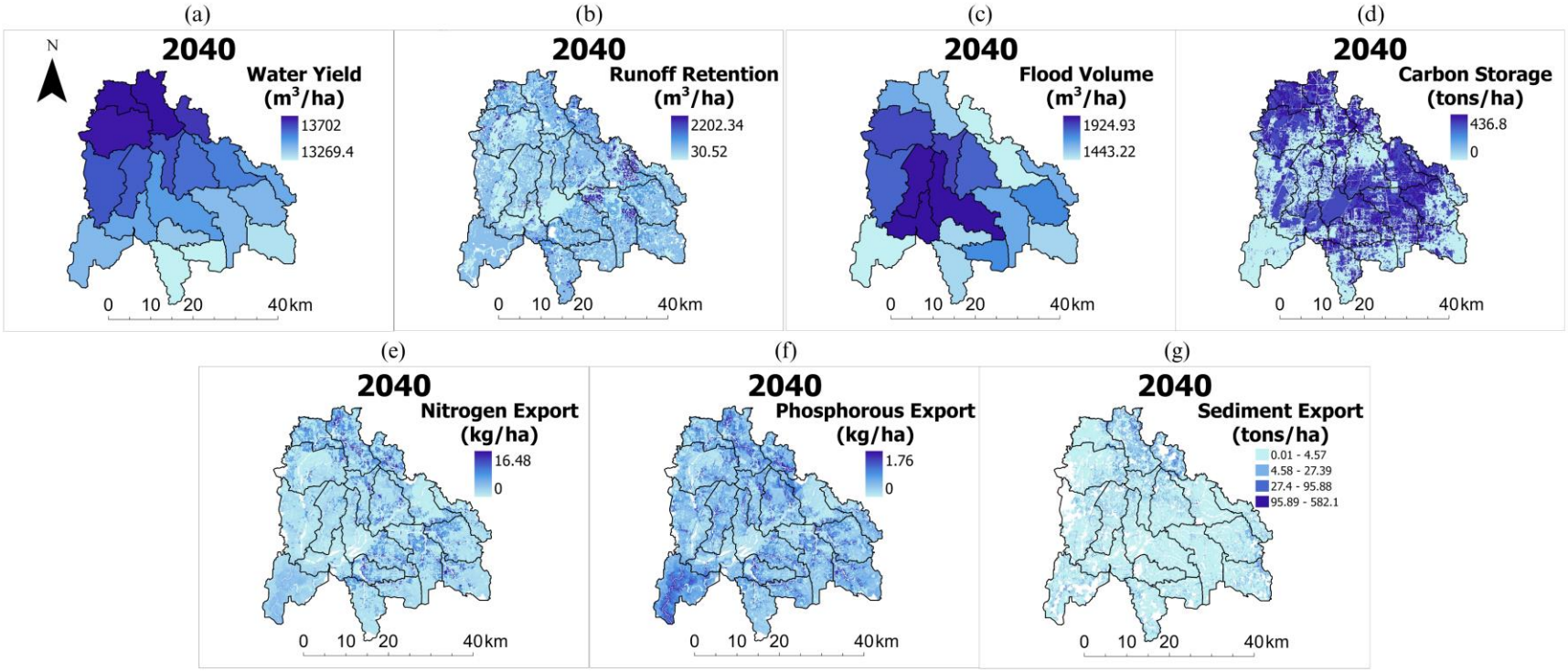
(a)
N
2040
Water Yield
(m³/ha)
13702
13269.4
0 10 20 40km
(b)
2040
Runoff Retention
(m³/ha)
2202.34
30.52
0 10 20 40km
(c)
2040
Flood Volume
(m³/ha)
1924.93
1443.22
0 10 20 40km
(d)
2040
Carbon Storage
(tons/ha)
436.8
0
0 10 20 40km
(e)
2040
Nitrogen Export
(kg/ha)
16.48
0
0 10 20 40km
(f)
2040
Phosphorous Export
(kg/ha)
1.76
0
0 10 20 40km
(g)
2040
Sediment Export
(tons/ha)
0.01 - 4.57
4.58 - 27.39
27.4 - 95.88
95.89 - 582.1
0 10 20 40km

(cont.)

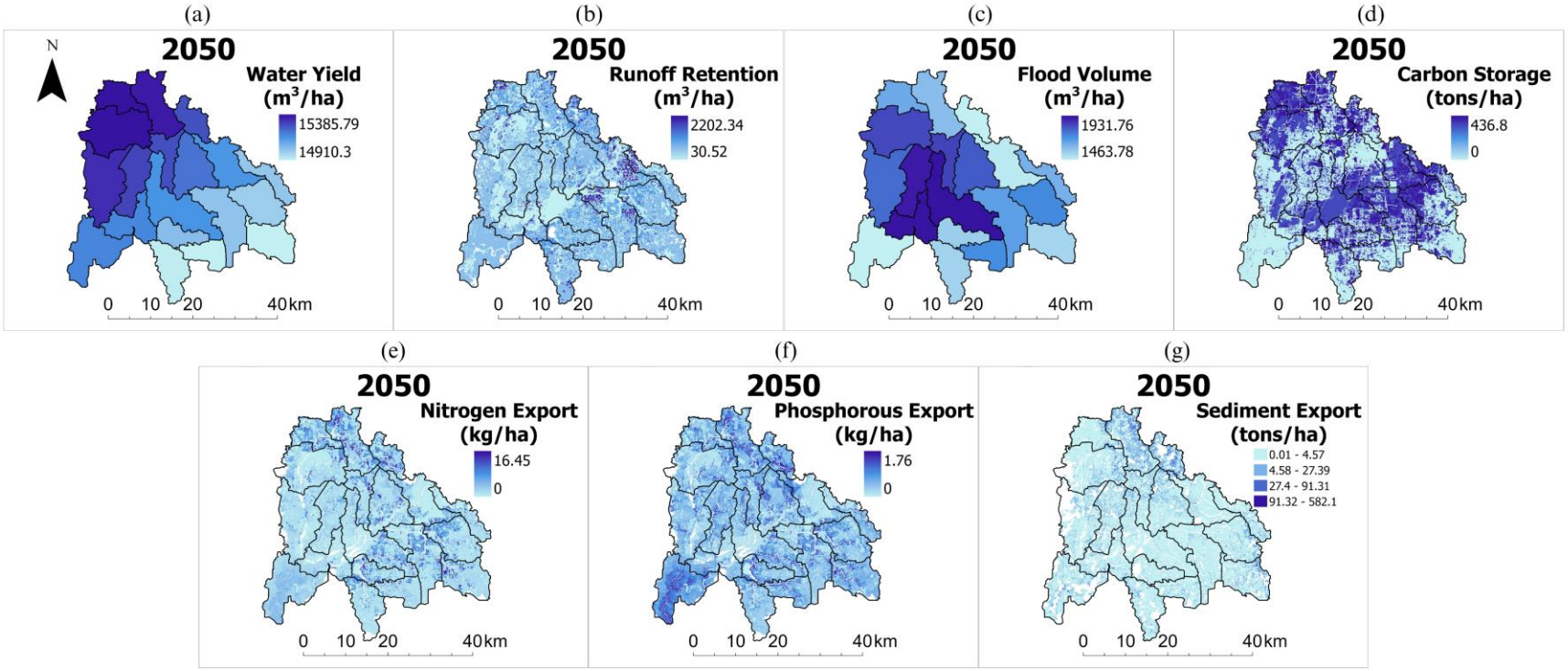

Figure S2. Spatial distribution of projected ecosystem service indicators for the years 2030, 2040, and 2050: (a) Water Yield (m³/ha), (b) Runoff Retention (m³/ha), (c) Flood Volume (m³/ha), (d) Carbon Storage (tons/ha), (e) Nitrogen Export (kg/ha), (f) Phosphorous Export (kg/ha), and (g) Sediment Export (tons/ha). Each map illustrates the spatial variation and magnitude of the respective indicators to support interpretation of future ecosystem service trends across the watershed.

Text S3.

The classification accuracy was evaluated using a confusion matrix derived from 1,885,526 reference pixels. The overall accuracy (observed agreement, p_o) was 96.07%, indicating that the vast majority of pixels were correctly classified. To further account for the possibility of agreement occurring by chance, Cohen's Kappa statistic was calculated. The expected agreement (p_e) was 0.298, yielding a Kappa value of 0.944. According to standard interpretation guidelines, a Kappa greater than 0.80 represents *almost perfect* agreement, confirming the robustness and reliability of the classification results.

Table S1. Cross-classification of actual and predicted LULC categories for the year 2023.

Value	Count	lulc2023 actual	Lulc2023 predicted
1	375824	6	6
2	12810	6	2
3	736396	2	2
4	112309	4	4
5	2435	6	4
6	1280	7	6
7	361	6	7
8	550673	7	7
9	13584	4	5
10	607	6	5
11	3118	7	2
12	1380	4	2
13	444	4	6
14	22345	2	6

15	1334	5	5
16	29523	1	1
17	866	1	7
18	2837	2	4
19	5394	3	3
20	96	6	1
21	24	5	7
22	444	5	6
23	614	5	4
24	908	1	6
25	22	7	4
26	1058	7	1
27	236	5	1
28	137	1	5
29	51	4	1
30	13	5	3
31	462	3	4
32	44	4	7
33	2434	2	7
34	26	7	5
35	2	4	3
36	26	6	3
37	233	1	3

38	307	3	2
39	1745	3	6
40	295	2	3
41	190	3	7
42	588	1	2
43	998	2	1
44	226	3	1
45	22	3	5
46	476	2	5
47	244	1	4
48	69	5	2
49	16	7	3

Table S2. Confusion matrix comparing actual and predicted LULC classes for 2023.

Actual \ Predicted	**1**	**2**	**3**	**4**	**5**	**6**	**7**	**Row Total**
1 (Water)	29,523	588	233	244	137	908	866	32,499
2 (Urban)	998	736,396	295	2,837	476	22,345	2,434	765,781
3 (Barren)	226	307	5,394	462	22	1,745	190	8,346
4 (Forest)	51	1,380	2	112,309	13,584	444	44	127,814
5 (Grassland)	236	69	13	614	1,334	444	24	2,734
6 (Cropland)	96	12,810	26	2,435	607	375,824	361	392,159
7 (Wetland)	1,058	3,118	16	22	26	1,280	550,673	556,193

Column Total	32,188	754,668	5,979	118,923	16,186	402,990	554,592	1,885,526

Diagonal sum=29,523+736,396+5,394+112,309+1,334+375,824+550,673=1,811,453

Observed agreement, p_o :

$$p_o = \frac{\text{Diagonal sum}}{N} = \frac{1{,}811{,}453}{1{,}885{,}526} \approx 0.9607 \text{ (or } 96.07\% \text{)}$$

Expected Agreement (p_e):

Kappa uses the idea of "random" agreement expected from row and column totals. Formally:

$$p_e = \frac{1}{N^2} \sum_{i=1}^{7} (\text{ RowTotal }_i \times \text{ ColumnTotal }_i).$$

So, for each class i, multiply its row total by its column total, sum all, then divide by N^2.

Row Totals = [32499, 765781, 8346, 127814, 2734, 392159, 556193]

Column Totals = [32188, 754668, 5979, 118923, 16186, 402990, 554592]

Computing each product:

1. $32499 \times 32188 = 1{,}046{,}077{,}812$
2. $765781 \times 754668 = 577{,}910{,}415{,}708$
3. $8346 \times 5979 = 49{,}900{,}734$
4. $127814 \times 118923 = 15{,}200{,}024{,}322$
5. $2734 \times 16186 = 44{,}252{,}524$
6. $392159 \times 402990 = 158{,}036{,}155{,}410$
7. $556193 \times 554592 = 308{,}460{,}188{,}256$

Summing up all products:

$$\sum_{i=1}^{7} (\text{Row}_i \times \text{Col}_i)$$

$$= 1{,}046{,}077{,}812 + 577{,}910{,}415{,}708 + 49{,}900{,}734 + 15{,}200{,}024{,}322 + 44{,}252{,}524$$
$$+ 158{,}036{,}155{,}410 + 308{,}460{,}188{,}256 = 1{,}060{,}747{,}014{,}766.$$

Next, $N^2 = (1{,}885{,}526)^2 \approx 3{,}555{,}208{,}296{,}676$.

Therefore,

$$p_e = \frac{1{,}060{,}747{,}014{,}766}{3{,}555{,}208{,}296{,}676} \approx 0.298.$$

Kappa Calculation:

The standard formula for Cohen's Kappa:

$$\kappa = \frac{p_o - p_e}{1 - p_e}$$

Plugging the numbers:

- $p_o \approx 0.9607$
- $p_e \approx 0.298$

$\kappa = \frac{0.9607 - 0.298}{1 - 0.298} = \frac{0.6627}{0.702} \approx 0.944$